Physics – Uspekhi **38** (6) 591 – 607 (1995)

PACS numbers: 11.15.Ha; 14.80.Hv; 74.20.De; 67.40.–w

Fractals, topological defects, and confinement in lattice gauge theories

M I Polikarpov

Contents

Abstract. Topological defects — monopoles, vortices, and strings — are discussed. It is shown that these objects form clusters with a nonintegral dimension, i.e. they are fractals. The fractal dimension reflects the physical properties of a system. In particular, studies of monopole current clusters in U(1) and SU(2) lattice gauge theories make it possible to identify the confinement mechanism. In the confinement phase the current lines of a magnetic monopole form a percolating cluster and these lines are so dense that their dimension exceeds unity, whereas in the deconfinement phase their dimension is trivial: it is equal to unity. It is also shown that the string tension is proportional to the dimension of extended monopole currents. This is in agreement with a confinement model based on the condensation of magnetic monopoles into a superconducting phase. A string between a quark and an antiquark is then analogous to an Abrikosov vortex in a superconductor. An account is given of the application of the theory of fractals in the problem of gauge fixing in lattice gauge theories. It is also demonstrated that, in SU(2) gluodynamics, domains of the deconfinement phase have a nonintegral dimension near a phase transition point. Apart from monopoles, the review deals also with the properties of vortex and string clusters in three-dimensional and four-dimensional XY models. The corresponding physical objects are vortices in liquid helium and 'global cosmic strings'.

M I Polikarpov Institute of Theoretical and Experimental Physics, B. Cheremushkinskaya 25, 117259 Moscow.
Tel. (7-095) 123 02 92. Fax (7-095) 123 65 84.
E-mail: polykarp@vxitep.itep.ru, polykarp@vxdesy.desy.de

Received 11 February 1995
Uspekhi Fizicheskikh Nauk **165** (6) 627 – 644 (1995)
Translated by A Tybulewicz

1. Introduction

Objects with a nonintegral dimension, i.e fractals, have been observed recently in very diverse fields of physics, mathematics, and biology [1]. This brief review will give examples of fractals found by numerical simulation of lattice gauge theories. Many interesting examples and rigorous definitions can be found in the well-known book of Mandelbrot [1] and in the review of Paladin and Vulpiani [2].

The main property of fractals is their nonintegral dimension. In reality, there is an infinite number of definitions of the fractal dimension, which give the same values for objects with an integral dimension, but generally give different values for fractals. This ambiguity in the definition of a nonintegral dimension is not very important. In specific applications the actual existence of a fractal is significant. A very simple definition of the dimension of a fractal will now be given by way of introduction. Let us consider an object consisting of a large number of points distributed in some way in a D-dimensional Euclidean space. Let us calculate the average number of points within a sphere of radius R (Fig. 1). To do this we can consider a function

$$f(R) = \frac{1}{N(N-1)} \sum_{i,j} \theta\big(R - |\boldsymbol{x}_i - \boldsymbol{x}_j|\big), \tag{1}$$

where N is the total number of points; $\boldsymbol{x}_i$ are the coordinates of these points; θ is the step function. If the investigated object is a fractal, then $f(R) \propto R^{D_{\rm f}}$ and the power exponent $D_{\rm f}$ can be regarded as the fractal dimension of the object. In the case of real examples there is a finite interval of the values of R in which the function f is proportional to the power exponent of R. Obviously, R should be (much) less than the size of the whole fractal, i.e. $R < L_{\rm f}$. It is also clear that R should be (much) greater than the minimum distance $l_{\rm f}$ between the

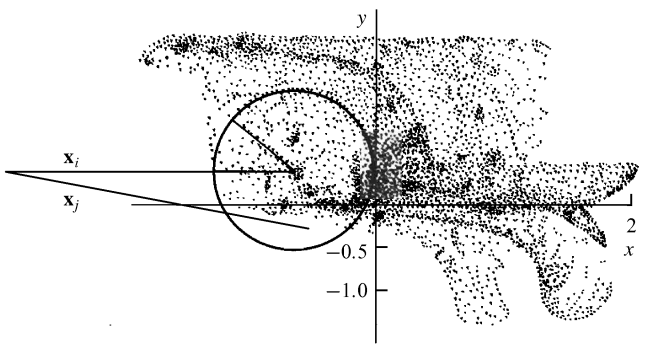

Figure 1. Calculation of the dimension of a fractal defined by the mapping operation (2).

points. The greater the number of points, the more accurate the precision of determination of the dimension D_f on the basis of the function (1). The very existence of a finite interval, where $f(R) \propto R^{D_f}$, reflects the fundamental property of fractals, which is their scaling invariance, i.e. self-similarity on different scales. More complex objects, multifractals, have less trivial properties [2]. Extensive material for computer games is provided by recursion equations: for example, the fractal shown in Fig. 1 is defined by the mapping operation

$$x^{\text{new}} = \sin(x^{\text{old}}) + \cos\left(\frac{1}{y^{\text{old}}}\right),$$
$$y^{\text{new}} = -\sin\left(\frac{1}{x^{\text{old}}}\right) + \cos(y^{\text{old}}). \tag{2}$$

Another simple example is the process of diffusion of N points ('bacteria') in which each point has a certain probability to 'multiply' or to 'die'. Fig. 2 is taken from Ref. [3] and it demonstrates the process for 500 points living on a plane. In the initial configuration the points are scattered at random on a square (Fig. 2a). At each step of the process half the randomly selected points disappear and the remaining points are 'doubled'; each point then shifts by a step proportional to a random number characterised by a Gaussian distribution of the probability (Brownian motion). Several islands or clusters form after 50 such steps (Fig. 2b). A large number of steps is followed by the survival of just one cluster which has a fractal dimension (Fig. 2c); all the points (bacteria) in this cluster have the same ancestor. It is interesting that the average linear size of this fractal is independent of the dimension of space (and is proportional to the square root of the total number of particles) and also that the centre of gravity diffuses at the rate of motion of one particle [3].

Reality (and the two examples given above) demonstrates that fractals appear almost always when even relatively simple systems are simulated numerically. In the case of physical models, the existence of fractals quite frequently reflects the existence of some nontrivial physical effect. An excellent example, found by Mandelbrot, is the application of fractals to the theory of turbulence [1, 2].

The aim of this review is to show that the 'fractal' concept is useful in the description of physical phenomena in lattice gauge theories. At the very least, a study of the fractal properties of vacuum in gluodynamics has helped

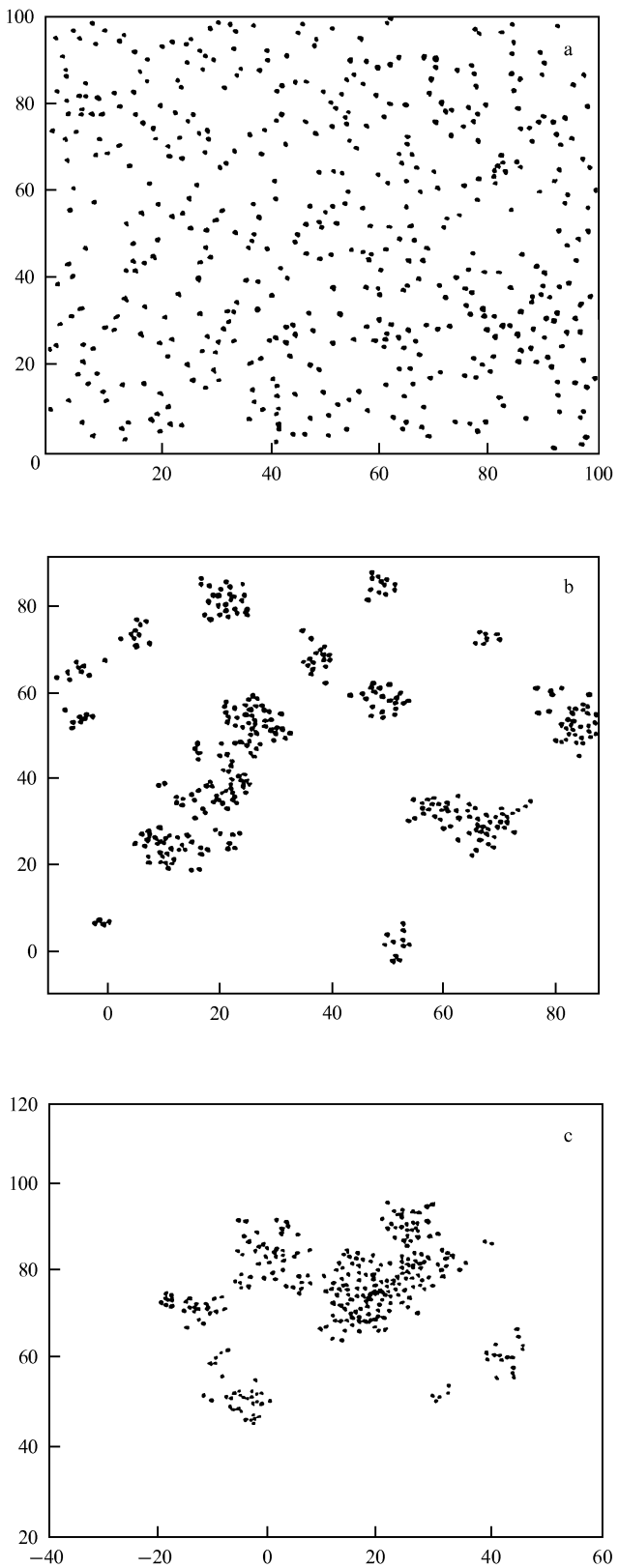

Figure 2. Evolution of an initially uniformly distributed set of points (a) by a diffusion process accompanied by reproduction, showing the configuration after 50 steps (b) and after 400 steps (c). At first sight it is quite surprising that the points do not 'spread out' over the plane, but occupy compact regions irrespective of the number of steps [3].

the author to understand the mechanism of colour confinement. Over 20 years ago it was suggested [4–6] that chromodynamics is a theory of strong interactions. However, one of the main problems which such a theory should tackle, which is the mechanism of colour confinement, has not yet been solved analytically. The reason lies naturally in the inability to treat theoretically a field theory with a large coupling constant. On the other hand, numerical calculations on a lattice reveal clearly a chromoelectric field tube between a static quark and a static antiquark (see, for example, Ref. [7]). In this review I shall show that numerical calculations make it possible to understand the confinement mechanism. The most popular theoretical explanation of confinement is based on a model proposed by 't Hooft and Mandelstam [8, 9] in which an electric field tube, formed between a quark and an antiquark, is a dual analogue of an Abrikosov vortex in a superconductor [10]. This requires that vacuum in this theory should be similar to a superconductor, but instead of a condensate of Cooper pairs there must be a condensate of monopoles. This vacuum is usually called a 'dual superconductor'.

In Section 3, I shall discuss how a similar confinement mechanism arises in compact electrodynamics. In particular, I shall show that the magnetic monopole currents form fractals [11] and that their dimension D_f plays the role of the order parameter for a confinement–deconfinement phase transition.

In Section 4, I shall consider the simplest non-Abelian theory on a lattice, which is SU(2) gluodynamics. It is not possible to understand intuitively the physical effects in non-Abelian theories, but the classical Abelian theories are well understood: there is a clear pattern of physical phenomena based on the Maxwell equations. Therefore, before considering the confinement in non-Abelian theories, it is necessary first to 'project' this phenomenon onto Abelian theories and then try to demonstrate the existence of a super-conducting phase of Abelian monopoles, which play the role of Cooper pairs. As in Section 3, a study of the lines of the magnetic monopole current will help to identify the confinement mechanism.

Section 5 deals with the problem of gauge fixing in lattice theories. In the case of compact fields, it is found that fixing even of such a simple gauge as $\partial_\mu A_\mu = 0$ is a nontrivial task and it will be shown that the fractal dimension is useful in tackling this task. Other examples of gauges, important in applications, will also be considered.

The fractal properties of vortices in the three-dimensional XY model and of 'global strings' in the four-dimensional XY model are described in Section 6.

The Appendix introduces the main concepts of lattice gauge theories, necessary for the understanding of the bulk of this review.

Section 2 deals with the fractal properties of deconfinement domains [12] in a gluon plasma in the region of a confinement–deconfinement phase transition. This simple example will serve to introduce definitions and concepts needed in the rest of the review.

2. Fractal properties of deconfinement domains

At sufficiently high temperatures ($T_c \sim 200$ MeV), a phase transition occurs in gluodynamics: a colour confinement phase changes to a deconfinement phase. In this section, based on the results of Ref. [12], I shall show that the deconfinement phase domains in SU(2) lattice gauge theory have a nonintegral dimension near the phase transition.

At a finite temperature a lattice theory is defined on an asymmetric lattice. The physical temperature on a lattice of size $N_s^3 N_t$ is related to the lattice step a as follows: $T = 1/N_t a$ (N_s is the size of the lattice along a spatial direction and N_t is the corresponding size along a time direction; the concept of temperature is definite if $N_s \gg N_t$). Since a depends on the unrenormalised (bare) charge g, it follows that temperature can be varied by altering N_t or g. My calculations were carried out on a lattice of $8^3 \times 4$ size. In the adopted theory the phase transition occurs at $4/g_c^2 \approx 2.32$ [13, 14]. The order parameter is a Polyakov line [15] and its quantum average is related to the free energy of a colour charge as follows: $L \propto \exp(-F/T)$. [By definition,

$$L = \frac{1}{2}\mathrm{Tr}\,\exp\left[\mathrm{i}\int_0^{1/T} \mathrm{d}t\, A_4(x)\right],$$

and in terms of the lattice notation

$$L(\boldsymbol{x}) = \frac{1}{2}\mathrm{Tr}\prod_{n=1}^{N_t} U_{x,4},$$

where $x = (\boldsymbol{x}, na)$]. Consequently, in the confinement phase, characterised by $F = \infty, \langle L\rangle = 0$, in the region of the phase transition we have $F < \infty$ and $\langle L\rangle \neq 0$.

It therefore follows that each site in the spatial lattice can be ascribed a value of L. A nonzero average $\langle L\rangle$ appears because the distribution of the values of L is asymmetric. By definition, we shall assume that a given lattice site lies in the deconfinement phase if the value of L corresponding to this site and averaged over six values of L corresponding to the neighbouring sites exceeds a certain value ε. It is assumed that the deconfinement phase occupies a unit cube, which belongs

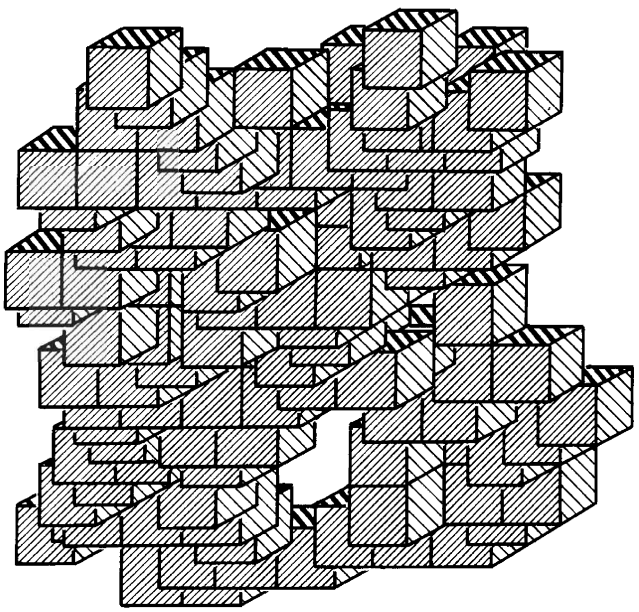

Figure 3. Example of a domain of a deconfinement phase in the SU(2) gluodynamics at a temperature close to the critical value: $T \approx 0.95T_c$.

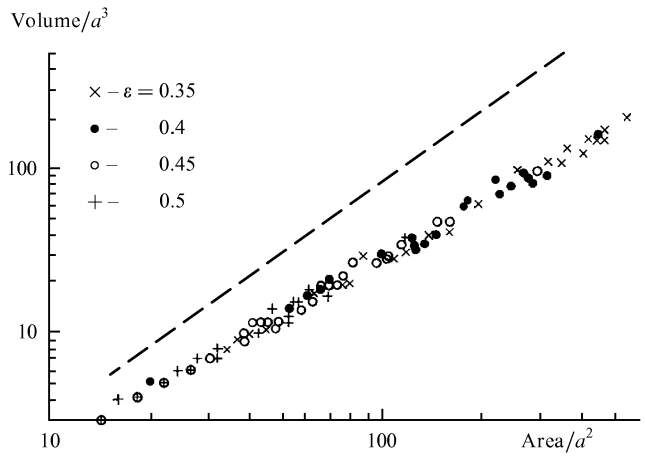

Figure 4. Dependence of the volume of deconfinement domains on the area of their surface. The dashed line is the dependence $V = \text{const} \times A^{3/2}$.

to a dual lattice†, and the point under consideration lies at the centre of this cube. If two cubes share a face, they are taken to belong to one domain. It follows that each configuration of fields corresponds to a certain number of three-dimensional domains of the deconfinement phase. The number and structure of these domains are governed in general by the value of the parameter ε, but it is found that variation of this parameter within a wide range does not influence the results significantly. In the confinement phase the shape of the domains is fairly simple: each consists of several cubes. Like the phase transition, the domain structure is fairly complex, as demonstrated by an example of a domain shown in Fig. 3.

Let us consider several lattice configurations of fields in the region of a phase transition and measure the volumes and areas of the deconfinement domains. The results obtained for $4/g^2 = 2.29$ are plotted in Fig. 4. The dependence of the volume on the area is described very well by the formula $V = \text{const} \times A^{\alpha}$, where $\alpha = 1.12 \pm 0.05$. The results agree within the limits of the error for $4/g^2 = 2.29$ ($T < T_c$) and for $4/g^2 = 2.35$ ($T > T_c$). If the domains are normal three-dimensional objects, then $V = \text{const} \times A^{3/2}$ and this dependence is represented by the dashed line in Fig. 4. It follows from this result that the domains have a 'loose' structure, which can be seen also in Fig. 3. A study of the fractal properties of domains [16–18], carried out near a phase transition in the three-dimensional Ising model, also gives a nontrivial power exponent $\alpha_I = 1.15 \pm 0.05$. This should be compared with $\alpha = 1.03 \pm 0.03$ obtained for our example when $g^2 = \infty$, i.e. for a random distribution of the values of L between -1 and 1. It should be stressed that if $g^2 = \infty$, regions with $L > \epsilon$ are not the deconfinement domains.

A calculation of the fractal dimension of the deconfinement phase domains, carried out on the basis of formula (1), shows that $D_f = 2.3 \pm 0.4$. We can see that the error in the determination of D_f is fairly large. In the case of objects on a lattice a much simpler definition of the fractal dimension can be proposed. The domains consist of unit cells (cubes) of a dual three-dimensional lattice. On the initial lattice, each domain corresponds to an object consisting of links and sites. The sites are at the centres of the cubes and the links intersect the shared faces of the adjacent cubes. The dimension of a cluster, which consists of lattice links, can be defined as the ratio of the number of links N_l to the number of sites N_s belonging to a cluster, i.e.

$$D_f = \frac{N_l}{N_s}. \tag{3}$$

The number of links on a periodic D-dimensional lattice is D times greater than the number of sites so that our definition gives the correct value of the dimension of an object occupying all the links on the lattice. In the case of lines of lower density a natural interpolation can be made between integral dimensions. Application of this definition to the deconfinement phase domains shows that $D_f = 2.5 \pm 0.2$ when $\epsilon = 0.4 - 0.45$. Calculations carried out by A I Veselov show that α depends weakly on temperature and is practically unaffected by a change from a lattice of $8^3 \times 4$ size to one of the $16^3 \times 4$ size.

3. Fractal dimension as a confinement–deconfinement order parameter

This section is based on the results reported in Ref. [11]. The usual order parameters, governing the phase of a gauge (confinement–deconfinement) field are the string tension σ [19] and the Polyakov line [15]. The string tension is the force acting between a quark and antiquark separated by an infinite distance. Therefore, the deconfinement phase is characterised by $\sigma = 0$ and the confinement phase by $\sigma \neq 0$. As pointed out above, in the case of the deconfinement phase we have $L \neq 0$ and for the confinement phase we have $L = 0$. The order parameter proposed here is associated with the confinement mechanism based on a model of vacuum in which a condensate of magnetic monopoles exists.

It is well known that in four-dimensional and three-dimensional compact quantum electrodynamics the confinement is indeed due to condensed monopoles [20–22]. In the next section we shall consider monopoles in four-dimensional compact lattice electrodynamics. The definitions introduced below will be useful in the next section in a discussion of a physically more interesting example of lattice gluodynamics.

Let us now consider the results of numerical calculations. Compact electrodynamics is a theory of Abelian gauge fields A_μ and the range of variation of these fields is finite. The actual range is unimportant and in lattice theories it is usual to assume that $-\pi < A_\mu a \leqslant \pi$ (a is the length of a lattice link). In four-dimensional compact lattice electrodynamics there is a confinement phase at high values of the charge (if $\beta < \beta_c$, where $\beta = 1/e^2$ and e is the unrenormalised charge). Since gauge fields are defined modulo $2\pi/a$, the field strength tensor — defined below by expression (5) — can have singularities which correspond to monopoles [21, 22]. In a continuum theory the charge inside the volume bounded by a surface S can be found from the Gauss theorem:

$$q = \frac{1}{4\pi}\int_S \boldsymbol{E}\cdot \mathrm{d}\boldsymbol{S} = \frac{1}{4\pi}\int_S F_{\mu\nu}\mathrm{d}^2\sigma_{\mu\nu}\,.$$

The same theorem applied to the dual field strength tensor gives the value of the magnetic charge

$$m = \frac{1}{8\pi}\int_S \epsilon_{\mu\nu\alpha\beta}F_{\mu\nu}\mathrm{d}^2\sigma_{\alpha\beta}\,. \tag{4}$$

† The 'dual lattice' concept is defined in the Appendix.

A nonzero value of m appears because of the presence of a singularity (Dirac string) in $F_{\mu\nu}$.

Before writing down a lattice analogue of the definition of a magnetic charge m, let us recall the definition of fields in lattice theories. In compact electrodynamics the dynamic variables θ $(-\pi \leqslant \theta < \pi)$ are defined on the lattice links. The variable $\theta_{x,\mu}$, corresponding to a lattice link emerging from a point x along a direction μ, is proportional to the vector potential $\theta_{x,\mu} = A_\mu(x)a$, where a is the length of a lattice link. Each plaquette (a unit square on a lattice) corresponds to a phase which is proportional to the field strength tensor:

$$\begin{aligned}\theta_{\mathrm{p}} &= \theta_{x,\mu} + \theta_{x+\hat{\mu},\nu} - \theta_{x,\nu} - \theta_{x+\hat{\nu},\mu} \bmod 2\pi \\ &= a^2 F_{\mu\nu}(x) + O(a^4)\,,\end{aligned} \tag{5}$$

where $\hat{\mu}$ is a vector of length a directed along the μ axis. The standard action of the theory has, in accordance with formula (18), the form $S = \beta(1 - \cos\theta_{\mathrm{p}})$.

Application of formula (4) to a unit three-dimensional cube on a lattice and replacement of integration over the surface by summation over the cube faces (on the assumption that a is small) gives

$$m = \frac{1}{4\pi}\sum_{\mathrm{p}} \theta_{\mathrm{p}}\,, \tag{6}$$

which is summed over the plaquette phases which correspond to the cube faces; their orientation is shown in Fig. 5. It is evident from this figure that each value of $\theta_{x,\mu}$ occurs twice in the sum (6): once with the plus sign and once with the minus sign; m can have a nonzero value only because mod 2π occurs in the definition of θ_{p} given by formula (5). In the case of noncompact fields there is no mod 2π in the definition of the field strength tensor and $m = 0$. This reflects the elementary fact of the absence of monopoles in noncompact electrodynamics. A discontinuity of 2π which appears for $m \neq 0$ on a plaquette corresponds to the formation of a Dirac string on a lattice. We can easily show that $m = 0, \pm 1, \pm 2$. The discrete values of the charge obey the Dirac quantisation condition. In four-dimensional space the monopoles

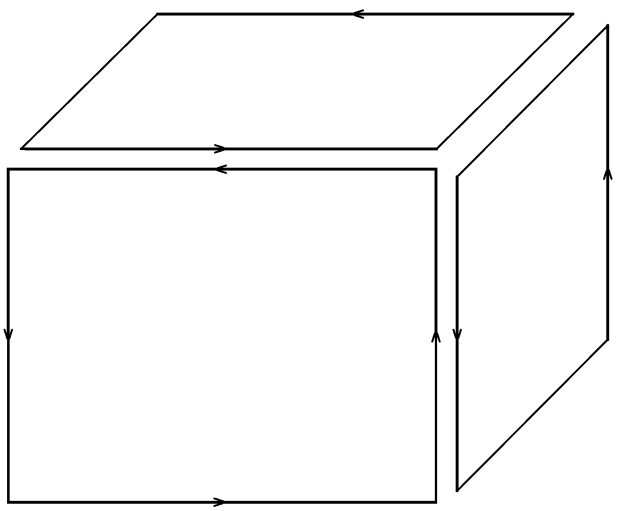

Figure 5. Going round the plaquettes which are the faces of a cube for which a magnetic charge is calculated from formula (6).

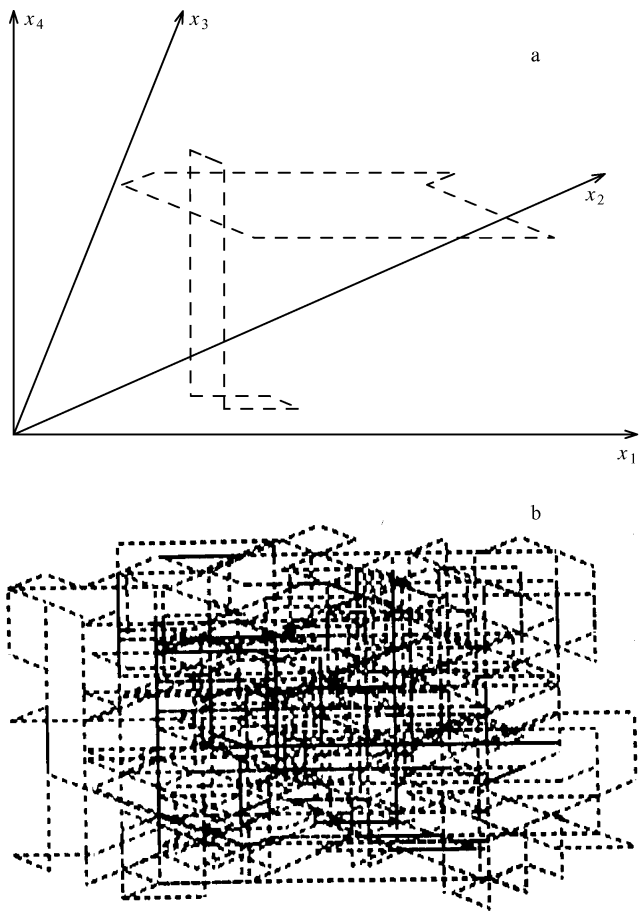

Figure 6. Lines of magnetic monopole currents in compact lattice electrodynamics: (a) deconfinement phase; (b) confinement phase.

correspond to the lines of a current which belong to the links of a four-dimensional dual lattice (a static monopole corresponds to a current directed along the 'time axis'). Any three-dimensional cube on a four-dimensional lattice corresponds to a link on a dual lattice. A cube is defined by three directions and a link dual to a cube is directed along the fourth direction. If a given three-dimensional cube corresponds to a magnetic charge m defined by formula (6), then a magnetic current ${}^*j = m$ flows along a dual link (see the Appendix). We can show that the lines of the current are closed and this naturally corresponds to the law of conservation of magnetic charges.

Numerical experiments [23–25] show that in the confinement phase the current lines cover densely a dual lattice and there are many self-intersections. In the deconfinement phase the current lines are less dense. Examples of the projections of the current lines from a four-dimensional space onto a two-dimensional surface of a page are shown in Figs. 6a and 6b for the deconfinement and confinement phases, respectively. Pictures of this kind were first given in Refs [24, 25].

It is found that a satisfactory language describing the currents of monopoles on a lattice is represented by the fractal dimension D_f defined by formula (3). Lattice fields have been generated and the lines of magnetic current have been identified for various values of β in lattice gauge U(1) theory. In each field configuration there are several connected objects (clusters). Fig. 7 shows the dependence

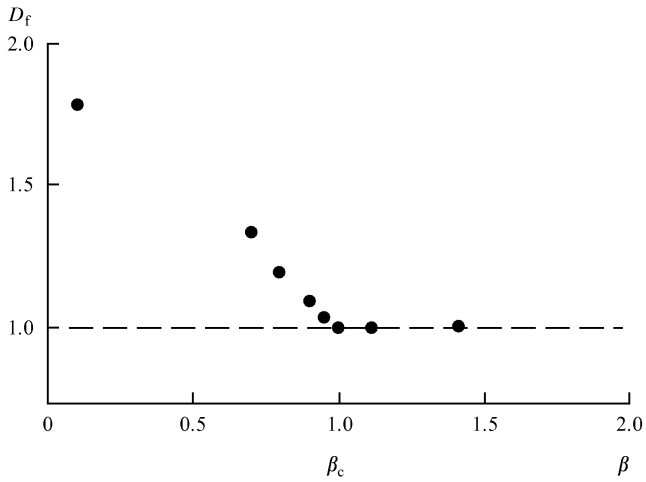

Figure 7. Dependence of the average dimension of the largest of clusters of magnetic monopole currents on β in compact lattice electrodynamics.

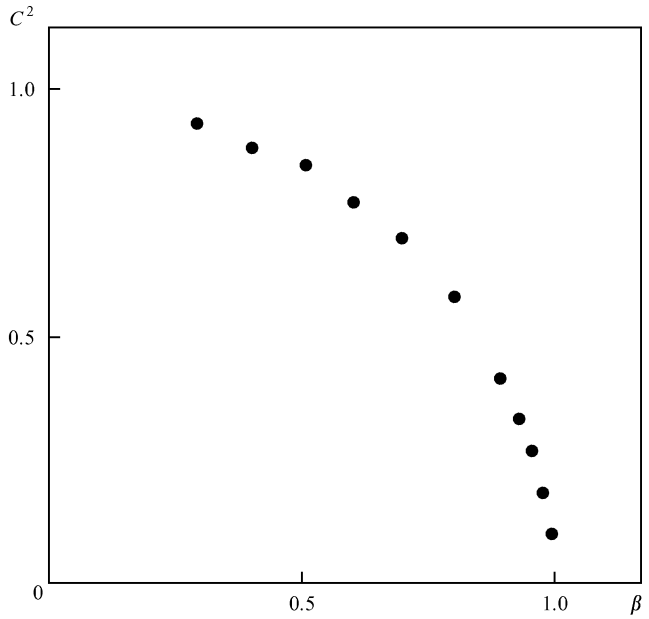

Figure 8. Square of the magnitude of the condensate of monopoles in compact lattice electrodynamics, calculated for a lattice of 10^4 size as a function of β.

of the average fractal dimension of the largest of the clusters on the value of β. We can see that in the confinement phase ($\beta < \beta_c$), the dimension D_f is nontrivial (an object composed of lines has the dimension $D_f > 1$). If $\beta > \beta_c$, then $D_f = 1$. The behaviour of the proposed order parameter D_f corresponds qualitatively to the pattern of condensation of magnetic monopoles in the confinement phase. The magnetic currents in the phase in which monopoles are condensed are so dense that their dimension is greater than unity. An even more direct numerical confirmation of the condensation of monopoles is given in Ref. [26], where a calculation of the effective potential of monopoles is reported; it is found that in the confinement phase this potential has a minimum corresponding to a monopole condensate (Higgs potential) and in the deconfinement phase the average value of the operator of creation of a monopole in vacuum is zero.

Finally, investigations [27, 28] of percolation properties [29, 30] of monopole clusters have shown that in the confinement phase there is a nonzero probability that two points are linked by a monopole current if the distance between them tends to infinity. In the deconfinement phase this probability is zero. Ten generated field configurations on a lattice of size 10^4 have been calculated for a given value of β and the probability that two points separated by a distance L are linked by a monopole current line has been found. This probability has then been fitted by the function:

$$f(L) = A\,\frac{\exp(-mL)}{L^{\alpha}} + C^4\,, \tag{7}$$

where A, α and C are fitting parameters. The dependence of C^2 on β is plotted in Fig. 8. If $\phi(x)$ is the monopole creation operator, the calculated probability is proportional to the correlation function $\langle\phi(0)\bar{\phi}(0)\phi(x)\bar{\phi}(x)\rangle$, and the parameter C represents a monopole condensate. An important consequence follows from Fig. 8: in the deconfinement phase, when $\beta > \beta_c$ (or in the confinement phase, when $\beta < \beta_c$), a monopole condensate is equal (or not equal) to zero, which is naturally in agreement with the confinement mechanism under discussion. A comparison of Figs 7 and 8 shows that the nontrivial fractal dimension (D_f) of monopole currents corresponds to the confinement phase in which monopoles are condensed. The quantity $D_f - 1$ behaves like the order parameter $D_f - 1 > 0$ for $\beta < \beta_c$ and $D_f - 1 \approx 0$ for $\beta > \beta_c$.

4. Abelian magnetic monopoles and confinement in gluodynamics

Partial gauge fixing in SU(N) gluodynamics which does not fix the gauge group $[\mathrm{U}(1)]^{N-1}$ is proposed in the well-known paper of 't Hooft [31]. The diagonal elements of a gluon field behave as gauge fields under residual Abelian transformations and the off-diagonal elements behave as matter fields. In view of the compact nature of the Abelian gauge group, there are monopoles in the system and if they are condensed, then confinement can be explained (as mentioned earlier) by a classical theory [8, 9]: vacuum behaves as a superconductor, the role of Cooper pairs is played by monopoles, and a string between the colour charges is a dual analogue of an Abrikosov vortex.

Many numerical experiments (discussed, for example, in Suzuki's review [32]) confirm the monopole confinement mechanism in the U(1) theory, derived by an Abelian projection from the SU(2) lattice gluodynamics. The string tension $\sigma_{\mathrm{U}(1)}$, deduced from the Wilson U(1) loops [which are the loops constructed only from the Abelian fields and the Abelian fields represent the projection of the SU(2) fields] is identical with the total string tension in the SU(2) gluodynamics [33]. There are indications [34] that the monopole density obeys the scaling law i.e. that monopoles survive in the continuum limit. The monopole currents satisfy the London equation for a superconductor [35]. It has also been shown recently [36, 37] that the string tension in the SU(2) gluodynamics can be reproduced by the contribution of the monopole currents. For complete clarity, it is very important to demonstrate the presence of a condensate of Abelian monopoles. It is known that in the confinement phase the density of monopoles is high and that it is low in the deconfinement phase [24, 25]. By itself, this does not yet prove the proposed confinement model. In

an ordinary conductor the density of free charges may be high but this is insufficient for the formation of an Abrikosov vortex: a charge carrier condensate is necessary.

We shall show in this section that in the SU(2) gluodynamics a monopole condensate, deduced (as described in the preceding section) from the percolation properties of magnetic currents, is — as expected — different from zero for the confinement phase and vanishes for the deconfinement phase [27, 28]. A numerical investigation of the effective action for monopoles [38] gives a similar result: the entropy of monopole currents is greater than their energy. Consequently, a monopole condensate exists in the SU(2) gluodynamics at absolute zero.

All these remarkable properties have been derived for just one, known as the maximum, Abelian projection [24, 25]. In fact, there is an infinite number of Abelian projections of a given non-Abelian theory. The confinement mechanism is found to depend on the projection. We shall show that a study of the fractal properties of the monopole currents demonstrates the special nature of the maximum Abelian projection.

Let us begin with the formal definition of an Abelian projection [31] and, for the sake of simplicity, let us consider the gauge group SU(2). An Abelian projection represents such partial fixing of the gauge of non-Abelian fields for which the Abelian calibration group remains nonfixed. The simplest example of such fixing is the diagonalisation of the field strength tensor $F_{\mu\nu}(x)$ for given values of μ and ν. In lattice theories the procedure is as follows. If a configuration of fields in a lattice $U_{x,\mu}$ is given, then for each lattice site an analogue of the field strength tensor is described by formula (A.2) in the Appendix. Under the gauge transformation given by formula (A.6), this matrix behaves as follows:

$$U'_{x,\mu\nu} = \Omega_x U_{x,\mu\nu} \Omega_x^+ . \tag{8}$$

For given values of μ and ν (for example, $\mu = 1$ and $\nu = 2$), it is possible to select for each lattice site the gauge transformation matrices Ω_x in such a way that $U'_{x,\mu\nu}$ is diagonal. Obviously, the transformation

$$\Omega_x \to \begin{pmatrix} \exp(\mathrm{i}\alpha_x) & 0 \\ 0 & \exp(-\mathrm{i}\alpha_x) \end{pmatrix} \Omega_x \tag{9}$$

leaves the matrix $U'_{x,\mu\nu}$ in the diagonal form. Therefore, the matrix Ω is defined, apart from the transformation given by the formula (9). The matrix elements of the fields $U_{x,\mu}$ which remain unfixed by this Abelian transformation are transformed as follows:

$$\begin{aligned} U^{11}_{x,\mu} &\to U^{11}_{x,\mu} \exp\left[\mathrm{i}(\alpha_x - \alpha_{x+\mu})\right] , \\ U^{12}_{x,\mu} &\to U^{12}_{x,\mu} \exp\left[\mathrm{i}(\alpha_x + \alpha_{x+\mu})\right] . \end{aligned} \tag{10}$$

The phase $\theta_{x,\mu}$ of a diagonal element $[U^{11}_{x,\mu} = \exp(\mathrm{i}\theta_{x,\mu})|U^{11}_{x,\mu}|]$ transforms as an Abelian gauge field on a lattice†: $\theta_{x,\mu} \to \theta_{x,\mu} + \alpha_x - \alpha_{x+\mu}$. The procedure for investigating monopole currents on a lattice in the SU(2) gluodynamics consists of the following steps:

(1) generation of configurations of the SU(2) fields with the weight $\exp(-S)$, where S is the SU(2) action;

(2) projection of the resultant SU(2) fields by, for example, diagonalisation of $U_{x,12}$ over the whole lattice, so that the phase of the diagonal elements $\theta_{x,\mu}$ can be regarded as an Abelian gauge field;

(3) calculation of the monopole currents in accordance with formula (6), as described in the preceding section.

The Abelian projection, which involves diagonalisation of $U_{x,\mu\nu}$, does not give interesting physical results. In fact, there is an infinite number of the SU(2)→U(1) projections. Instead of a plaquette matrix, which becomes diagonalised by the gauge transformation, we can select any operator which transforms in a manner similar to that described by formula (8): $X(x) \to \Omega_x X(x) \Omega_x^+$. For example, at a finite temperature we can diagonalise a Polyakov line

$$L(x) = \prod_{i=1}^{N} U_{x+(i-1)\cdot\hat{\mu},\mu} , \qquad \mu = 4 ;$$

We can easily see that this line behaves under gauge transformations in exactly the same way. Another example is the maximum Abelian projection [24, 25], which corresponds to the search for the next maximum:

$$\max_{\Omega_x} \sum_{x,\mu} \mathrm{Tr}\,(U'_{x,\mu}\sigma_3 U'^{+}_{x,\mu}\sigma_3) . \tag{11}$$

Here $U'_{x,\mu}$ is the gauge-transformed field given by formula (A.6) and the sum is taken over all the lattice links. We can easily see that this projection makes the $U_{x,\mu}$ gauge fields as diagonal as possible and hence its name. Obviously, condition (11) is invariant under the Abelian transformations (9) and the phase of $(U'_{x,\mu})^{11}$ plays the role of a compact gauge field from which monopoles can be formed in a certain configuration. As pointed out at the beginning of this section, it is the maximum Abelian projection that provides much evidence that the vacuum in the SU(2) gluodynamics is constructed in a way similar to a dual superconductor and the monopoles formed from the fields $\theta_{x,\mu}$ are condensed.

Apart from ambiguities in the selection of the projection of a non-Abelian theory on an Abelian one, there is also ambiguity in the U(1) theory itself [39]. We can assume that

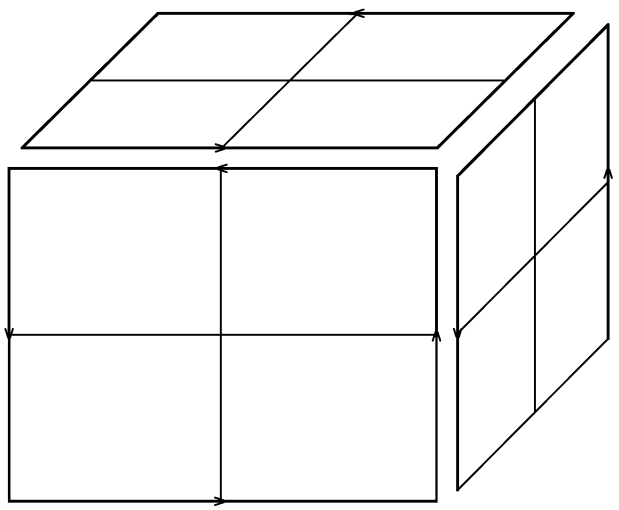

Figure 9. Construction of an extended monopole.

† In the continuum limit the diagonal elements of a gauge field also transform as the Abelian gauge fields: $A^{ii}_\mu \to A^{ii}_\mu + \mathrm{i}\,\partial_\mu\alpha$; the off-diagonal elements transform as the matter fields of charge 2: $A^{\pm}_\mu \to A^{\pm}_\mu \exp(\pm 2\mathrm{i}\alpha)$.

the SU(2) theory is projected on the U(1) theory with link lengths a, $2a$, ... This means that the monopoles described by formula (6) can be obtained by summing the phases not only of the elementary plaquettes (see Fig. 5), but also the phases of contours of size $2a$ (Fig. 9), $3a$, ... Such 'extended' monopoles [39] of 2^3, 3^3, ... size may possibly play an important role in the formulation of the gluodynamics action in terms of monopole currents [40].

It is found that the fractal dimension of monopole currents is proportional to the string tension σ (which is the force acting between a quark and an antiquark separated by an infinite distance) and the magnitude of the monopole condensate is correlated with the string tension. Two methods have been used to vary the string tension [27, 28, 39]: the first is more physical and involves variation of temperature, whereas the second is more formal and is known as the cooling of gauge fields.

Fig. 10 gives the temperature dependence of the magnitude of a condensate of monopoles. The calculations used in this figure [27, 28] have been carried out for the SU(2) gluodynamics on a lattice of $10^3 \times 4$ size. The magnitude of the condensate has been calculated on the basis of percolation properties of the monopole currents [see the explanation following formula (7) in the preceding section]. The monopole currents have been obtained on the basis of the maximum Abelian projection. Fig. 10 includes also the values of the string tension σ reported in Ref. [41]. We can see that the condensate and the string tension vanish at the critical point $T = T_c$. The same result is obtained in Ref. [28] also for the monopoles of 2^3 and 3^3 size. The fractal dimension of the monopole currents 1^3, 2^3, and 3^3 is greater than unity if $T < T_c$ (in the confinement region) and is trivial ($D_f = 1$) if $T > T_c$. Therefore, the percolation properties of monopole clusters and their fractal dimension, obtained by the maximum Abelian projection in the SU(2) gluodynamics at a finite temperature, support the monopole confinement mechanism.

Similar results are reported in Ref. [39] when the string tension is varied by the method in which vacuum fields are cooled. This method [42–45] involves consecutive variation of the link matrices $U_{x,\mu}$ in such a way that each variation minimises the action. Therefore, every time a local minimum is sought, the global minimum (when $U_{x,\mu} = 1$ for all x and μ) is obtained after several tens or even hundreds of passes through all the lattice links. In the first few steps the string tension is almost constant [46] and the subsequent cooling steps reduce this tension [47]. Therefore, the cooling procedure makes it possible to vary smoothly the string tension. If the initial configuration of the fields has a distribution with the probability density $\exp(-S)$, then after the very first field-cooling step the distribution is different. This cooling procedure can be regarded as motion, in the configurational space, of fields over a certain path which connects the quantum fields to the vacuum field $A_\mu = \Omega^+ \partial_\mu \Omega$.

Fig. 11 shows the dependence [39] of the fractal dimension of the monopole currents on the string tension obtained by the maximum Abelian projection in the SU(2) gluody-namics. The initial SU(2) field configurations have been obtained by the Monte Carlo method on a lattice of 10^4 size for an unrenormalised charge $g^2 \approx 1.78$. These configurations have then been cooled and at each cooling stage the maximum Abelian projection has been fixed and the fractal dimension of the monopole currents as well as the string tension have been calculated. We can see that the fractal dimension of the monopole currents of size 1^3, 2^3, and 3^3 is proportional to the string tension. This correlation is one further proof of the monopole confinement mechanism. It should be pointed out that monopoles of size 1^3

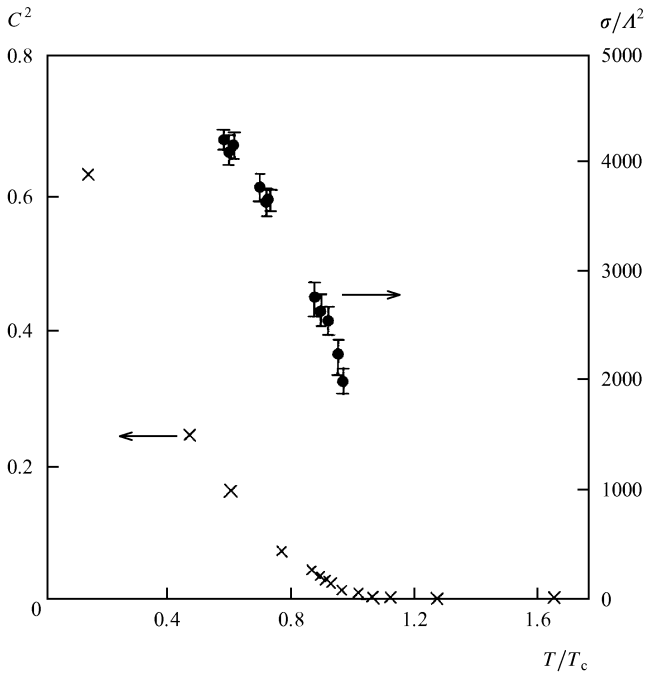

Figure 10. Temperature dependences of the square of the magnitude of the condensate of monopoles (×) and of the string tension (•) in the SU(2) gluodynamics.

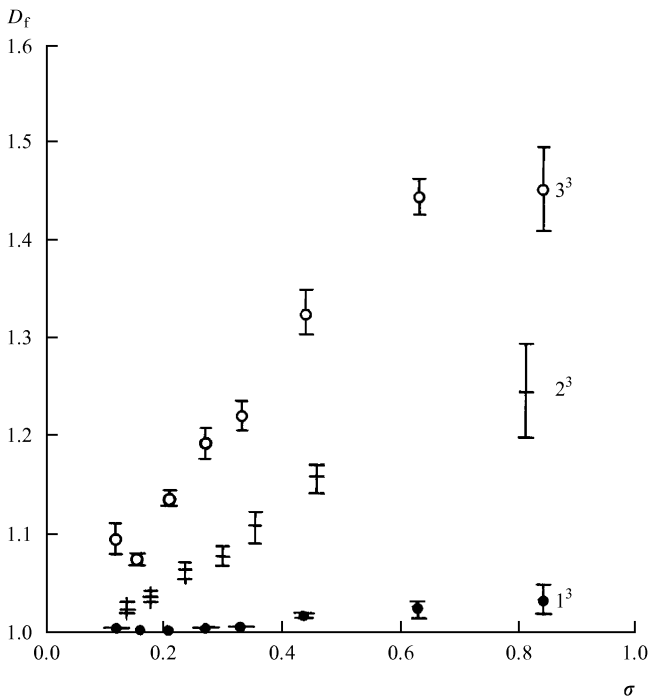

Figure 11. Dependence of the fractal dimension of monopole currents of size 1^3, 2^3, and 3^3 on the string tension during cooling. The monopoles are obtained from the maximum Abelian projection in the SU(2) gluodynamics.

rapidly disappear as a result of cooling and numerical estimates demonstrate that their density is far too low to account for the string tension. It follows that in the 'cooled vacuum' the confinement is due to extended monopoles of size 2^3, 3^3, ... The role of extended monopoles in the confinement mechanism is now under active investigation. The results mentioned above indicate that extended monopoles are important in the case of lattice links of finite length (since our results have been obtained for one value of the unrenormalised charge g); it is important to know the size of the monopoles responsible for the confinement in the continuum limit. These monopoles may be finite (of the order of the confinement radius) or they may be of zero size.

Fig 12, fully analogous to Fig. 11, gives the dimension of the monopole currents as a function of the string tension [39]. In this case each cooling step has involved the Abelian projection, corresponding to the diagonalisation of the plaquette matrix $U_{x,12}$ described by formula (A.2). Obviously, in the case of this Abelian projection the fractal dimension is not proportional to the string tension and there are serious reasons indicating that the monopoles are no longer responsible for the confinement. A detailed discussion of the special nature of the maximum Abelian projection is provided in Ref. [48]. It is found that in the lattice gluodynamics there is an example of an Abelian projection ('minimum Abelian projection') in which the confinement is not due to monopoles, but to 'minopoles' which are topological objects constructed from the off-diagonal elements of the lattice fields $U^{12}_{x,\mu}$. We recall that the monopoles are obtained from the phase of the diagonal elements $U^{11}_{x,\mu}$.

A detailed discussion of the confinement mechanism for an arbitrary Abelian projection is outside the scope of this review. It should be pointed out, however, that in general both the diagonal fields $U^{11}_{x,\mu}$ [U(1) gauge fields] and the off-diagonal fields $U^{12}_{x,\mu}$ [U(1) matter fields] may be responsible for the confinement [48–50]. We can assume that there is some object responsible for the confinement and described in a natural way in terms of the SU(2) fields and that the monopoles obtained by the maximum of Abelian projection reduce to this object. In the case of other Abelian projections, this object may transform into topological defects constructed from both the diagonal and off-diagonal elements of the fields $U^{11}_{x,\mu}$ and $U^{12}_{x,\mu}$. The most probable candidate [51] is the classical solution of the dyon type [52–55]; dyons of different sizes can be identified with extended monopoles of different sizes. My own preliminary numerical experiments have confirmed this behaviour. The conclusion that follows from this section is as follows: although many details are still not clear, it is obvious that numerical investigation of lattice gluodynamics has made it possible to establish the general features of the colour confinement mechanism: in the maximum Abelian projection the vacuum behaves like a dual superconductor.

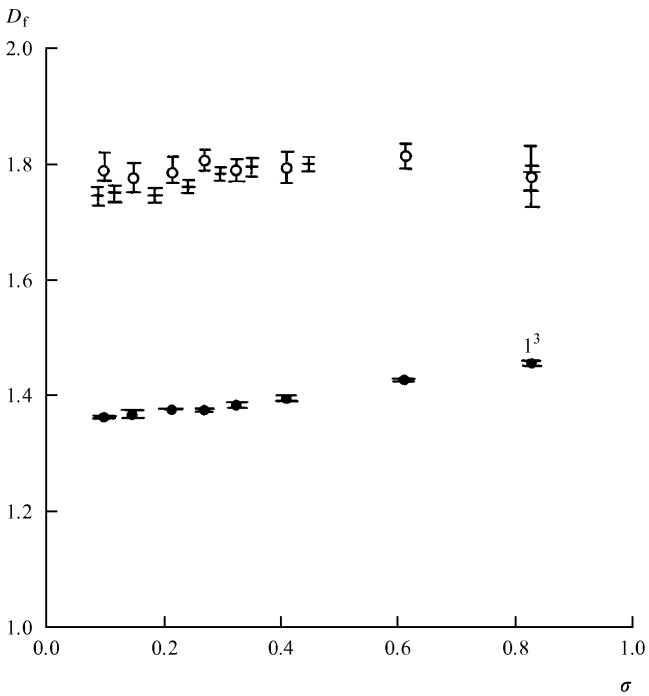

Figure 12. Same as in Fig. 11, but monopoles obtained from that projection in the SU(2) gluodynamics which corresponds to diagonalisation of the plaquette matrix.

5. Gauge fixing in lattice theories

The gauge-invariant quantities are of obvious physical interest, but there have been a large number of papers in which lattice gauge fields have been studied in chromodynamics and gluodynamics for a fixed gauge (see, for example, Ref. [56] and the literature cited there). The task of projecting a non-Abelian group on an Abelian one, described in the preceding section, is also technically very close to gauge fixing. In this section we shall show how the theory of fractals is applied to the problem of gauge fixing.

It is quite simple to fix the gauge $A_0 = 0$ in a lattice theory with free boundary conditions. However, the lattice analogue of the Landau gauge ($\partial_\mu A_\mu = 0$) is not trivial even in compact electrodynamics, since the problem is strongly nonlinear. The correct lattice formulation of the Landau gauge is the search for the following maximum:

$$\max_{\Omega_x} \sum_x F(x)\,, \qquad F(x) = \sum_{\mu=1}^{D} \mathrm{Re\,Tr}\,(\Omega_x^+ U_{x,\mu} \Omega_{x+\hat{\mu}})\,. \qquad (12)$$

The differential condition for an extremum, corresponding to this maximum, reduces in the continuum limit to $\partial_\mu \hat{A}_\mu = 0$. Condition (12) is nonlocal and in numerical calculations a computer program involves many passes through all the points on the lattice with maximisation of $F(x)$ at each point; this means that only Ω_x is varied and the remaining values of Ω_y $(y \neq x)$ are fixed. The procedure converges rapidly, but it is found that at some points x the function $F(x)$ is maximised much less satisfactorily than at the majority of other points on the lattice.

By way of example, we shall give the results of Ref. [57] in which the Landau gauge has been fixed for fields in three-dimensional compact electrodynamics, derived for a charge $e^2 = 1/2.3$ on a lattice of 25^3 size. After gauge fixing a typical value of the function $F(x)$ is of the order of 0.95. However, at 3% of the points this function is $F(x) < 0.77$. The points at which the gauge fixing is difficult are represented in Fig. 13 by small circles, taken from Ref. [57]. Determination of the fractal dimension of the regions formed by these points shows that $D_f \sim 1$. Since in three-dimensional electrodynamics the only known one-dimen-

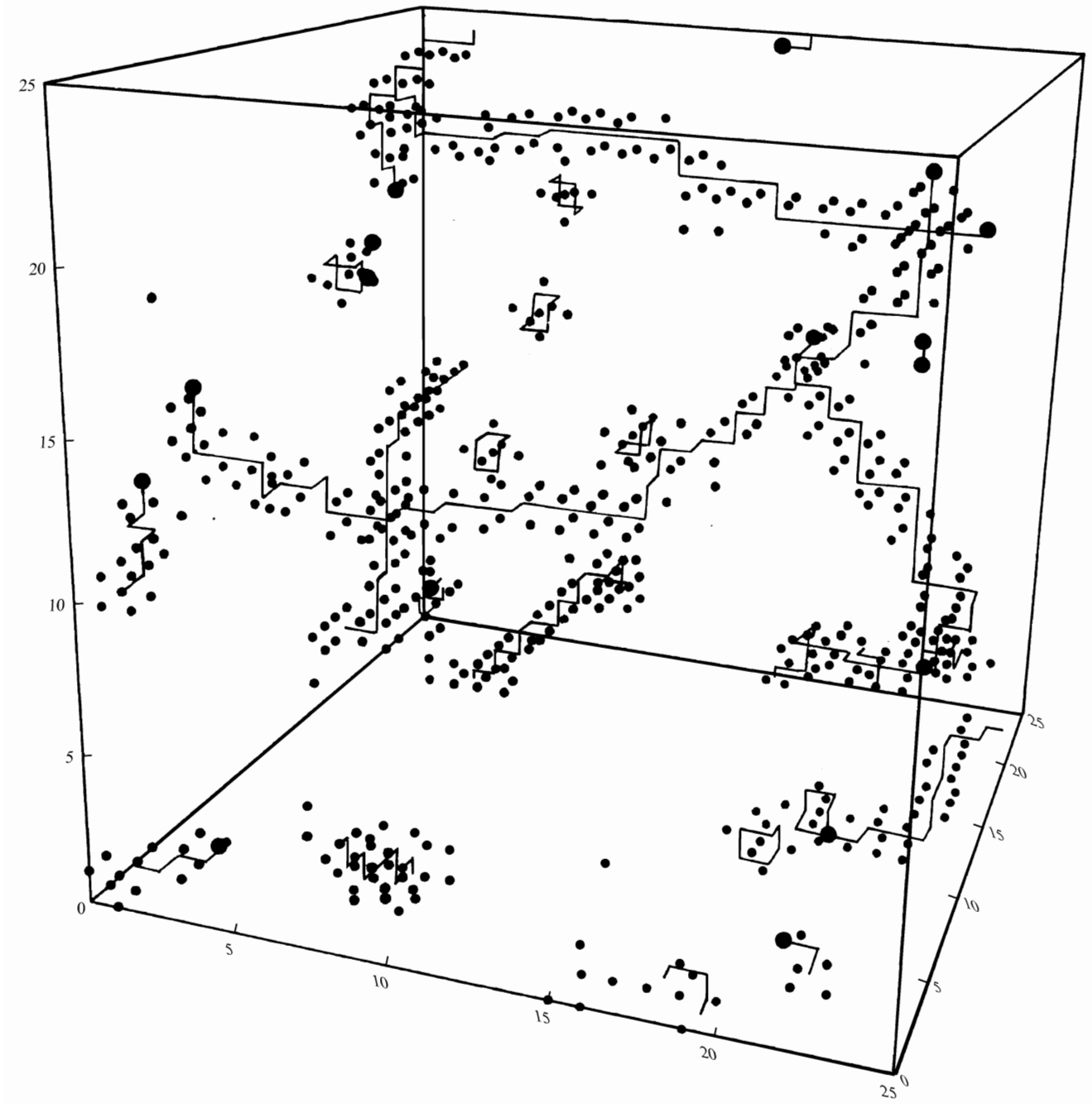

Figure 13. Typical configuration of fields in three-dimensional compact electrodynamics on a 25^3 lattice. The small dots represent the regions where the Landau gauge is poorly fixed and the large dots are the positions of monopoles. The lines represent the Dirac strings which occupy a fixed position for the fixed gauge.

sional objects are the Dirac strings (which occupy specific positions when the gauge is fixed), it is easy to guess that these objects are specifically responsible for regions with small values of $F(x)$ (i.e. regions where it is difficult to fix the gauge). The continuous lines in Fig. 13 are the Dirac strings, whereas the large dots are monopoles and antimonopoles. Periodic boundary conditions are superimposed on the lattice so that the Dirac strings, which apparently are discontinuous, are in fact either closed or they begin at monopoles and end at antimonopoles. If a Dirac string is directed along the z axis, its vector potential in cylindrical coordinates is

$$A^{\mathrm{str}} = \vec{\phi}\,\frac{1}{\sqrt{x^2+y^2}}$$

when a monopole is located at the origin of the coordinate system, whereas in the case of spherical coordinates the corresponding expression is

$$A^{\mathrm{mon}} = \vec{\phi}\,\frac{1-\cos\theta}{r\sin\theta}\,.$$

It is clear that singularities of the Dirac strings and monopoles hinder gauge fixing.

The Landau gauge has also been investigated on a lattice for the SU(3) gluodynamics [56]. The circles in Fig. 14 give the fractal dimension of the objects formed by the

points at which there are difficulties with gauge fixing. A calculation of the function $f(R)$ based on the function (1) is used in the dependence† plotted in Fig. 14:

$$D_{\mathrm{f}} = \frac{\partial \ln f(R)}{\partial \ln R} \,. \tag{13}$$

In the range $R < R_{\max} \sim 1.2$, a plateau with $D_{\mathrm{f}} \sim 1$ is clearly visible; at higher values of R the dimension D_{f} tends to the dimension of the lattice, which is 4. This behaviour of D_{f} shows that there are objects with the dimension close to unity; the linear size of these objects is less than $2R_{\max} \sim 2.5$. Objects are distributed at random over a lattice and, therefore, if the value of R is large (in excess of the linear size of the objects), D_{f} tends to the dimension of the lattice, which is 4. The stars in Fig. 14 give the dimension D_{f} deduced from formula (13) for points scattered at random over the lattice. We can see that D_{f} increases smoothly from zero to 4 when R is increased from zero to $R_1 \sim 11.5$. There is no plateau at low values of R and when R exceeds the average distance between the points ($R \geqslant R_1$), the value of D_{f} becomes approximately equal to the dimension of the lattice, which is 4. The value of R_1 from which D_{f} begins to reach a plateau for randomly scattered points naturally depends on the density ρ of these points. The value of ρ is selected here so that R_1 is of the order of $R_{\max}$.

In the case of the maximum Abelian projection $\mathrm{SU}(N) \to [U(1)]^{N-1}$ [24, 25, 31], discussed in the preceding section, there are also regions on a lattice where the maximum described by formula (11) is reached with greater difficulty than for the majority of the points on the lattice. The dimension of this region is calculated from formula (13) and is represented by crosses in Fig. 14. We can see that D_{f} behaves in the same way as in the case of a random distribution. All the results presented in Fig. 14 are obtained in Ref. [56] by an analysis of eight independent configura-tions of SU(3) fields on a lattice of $24^3 \times 40$ size for $g^2 = 1$ (g is the unrenormalised charge on the lattice).

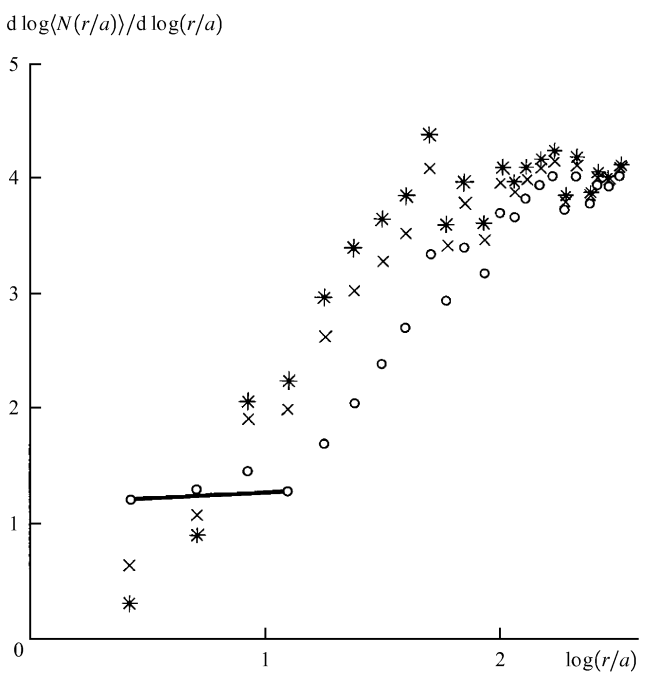

Figure 14. Fractal dimension of regions where the Landau gauge is poorly fixed in the SU(3) gluodynamics (○). The line is drawn in the part of the plateau that corresponds to $D_{\mathrm{f}} \approx 1$. Similar results for the maximum Abelian projection (×) have no such plateau. The results for randomly distributed points (∗) are included for the sake of comparison.

† In this section we shall assume that each lattice step a is unity.

It therefore follows that fixing of the Landau gauge in accordance with formula (12) selects certain one-dimensional objects in the four-dimensional SU(3) gluodynamics. The maximum Abelian projection leads to point objects scattered at random on a lattice. The physical meaning of one-dimensional or point objects is not yet clear. It is possible that one-dimensional objects are related to the confinement dynamics, as shown in Ref. [56], and that they are sensitive to a thermal phase transition. In the confinement phase the tangling up of the lines makes the dimension of the objects greater than unity ($D_{\mathrm{f}} \sim 1.3$ for $T \leqslant T_{\mathrm{c}}$) and at a phase transition point the dimension changes abruptly and becomes $D_{\mathrm{f}} \sim 1$ for $T \geqslant T_{\mathrm{c}}$.

6. Vortices and strings in the XY model

The monopoles discussed in the preceding sections are point objects: their dynamics in the four-dimensional spacetime is governed by one-dimensional monopole world lines. In this section we shall discuss string-like objects which correspond to world surfaces in four-dimensional spacetime. We shall consider defects corresponding to 'global cosmic strings' [58]. Nonperturbative investigation of these objects may be important, because cosmic strings could be responsible for the following scenario of the formation of galaxies. At high temperatures (in the early Universe) the U(1) symmetry is unbroken and there is a string condensate. This is possible because the string tension is zero in this phase and the formation of a closed string does not require energy. The condensed strings form clusters in the Universe and their size is of the order of the size of the Universe itself (percolation effect). A phase transition, corresponding to breaking of the U(1) symmetry, occurs when temperatures are lowered. A nonzero string tension appears and strings become massive objects. Tiny closed strings 'collapse' and decay into Goldstone bosons. Strings of size of the same order as the Universe become 'frozen' and form stable massive structures on which accretion of cosmic dust takes place, leading to the formation of galaxies. The general cause of the appearance of topological defects is the compact nature of the dynamic variables. If in a D-dimensional space there is a field of dimension‡ k, then the dimension of the corresponding defect, existing on a dual lattice, is $D - k - 2$ [59, 60]. In the XY model considered in the Appendix the compact dynamic variable is the scalar field φ_i locked to lattice sites i and characterised by $k = 0$. Therefore, as discussed in the Appendix, the dimension j of a defect described by formula (A.13) is zero for $D = 2$, 1 for $D = 3$, and 2 for $D = 4$. In the case of compact electrodynamics, we have $k = 1$ and $D = 4$ and the

‡ We shall discuss here the fields which are antisymmetric tensors of rank k; for a scalar field, we have $k = 0$ and the field is locked to a lattice site; in the case of a gauge field associated with an edge, we have $k = 1$; for a 'hyperfield' $h_{\mu\nu}(x) = -h_{\nu\mu}(x)$, associated with a plaquette, we have $k = 2$, and so on.

dimension of a defect (monopole current) is unity, as expected. The well-known Berezinskii–Kosterlitz–Thouless transition [61, 62] in the two-dimensional XY model is due to zero-dimensional vortices. It will be shown in the next section that for $D = 3$ and $D = 4$ the dynamics of one-dimensional and two-dimensional vortices is also closely related to a phase transition.

The lattice XY model is a discretised variant of the theory of the scalar field Φ with broken-down global U(1) symmetry. The potential in this field theory is $\lambda(|\Phi|^2 - \Phi_0^2)^2$, and, in the limit $\lambda \to \infty$, the radial part $|\Phi|$ becomes frozen, whereas the remaining dynamic variable φ is compact $[\Phi = |\Phi_0| \exp(\mathrm{i}\varphi)]$. In reality, only the kinetic part of the field φ remains. The lattice action, given by formula (A.12) in the XY model represents in fact the kinetic energy of the field φ; the cosine in the action described by formula (A.12), which takes into account the compact nature of the relationship, can be replaced by any 2π-periodic function such that

$$f(x) \underset{x \to 0}{\longrightarrow} \text{const} \times x^2 .$$

The last condition means that in the continuum limit $(a \to 0)$ the lattice action S is converted to the continuous action

$$\beta \int (\nabla\varphi)^2 \, \mathrm{d}^D x .$$

'Global strings' occur in the scalar theory with broken-down global U(1) symmetry and these strings correspond exactly to topological defects in the lattice XY model, considered in the Appendix. In fact, in going round the string the scalar field Φ acquires an additional phase 2π [58]. This corresponds to going round on a plaquette (Fig. 15), which leads to a defect with $j \neq 0$ described by formula (A.13), since φ is the phase of the field Φ.

It follows that in the four-dimensional XY model the topological defects are global strings, whereas in the three-dimensional XY model the topological defects are vortices in the three-dimensional scalar theory, such as vortices and liquid helium below the λ point [63, 64]. In the three-dimensional model the defects should be considered also as specific configurations of spins in a three-dimensional crystal.

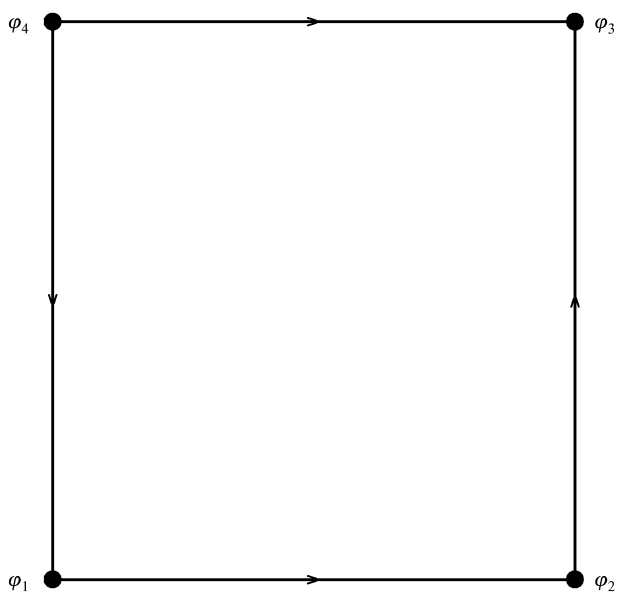

Figure 15. Plaquette and scalar variables φ_i .

We shall now describe the results of numerical calculations carried out in the XY model framework. For $D = 3$, in the model given by formula (A.12), there is a phase transition when $\beta_c \approx 0.4542$ [65, 66], but if $D = 4$, such a transition occurs for $\beta_c \approx 0.32$ [60].

For $D = 3$ and $D = 4$ the fractal properties of vortices and strings are exactly the same as in the case of monopole lines in electrodynamics (Section 3) and in gluodynamics (Section 4). Below the phase transition $(\beta < \beta_c)$ the dimension is nontrivial. For world surfaces of strings we have $D_f > 2$, whereas for vortices, we obtain $D_f > 1$; if $\beta > \beta_c$, both vortices and strings form clusters with a simple geometry: $D_f = 2$ for the world surfaces of strings $(4DXY)$ and $D_f = 1$ for the vortices $(3DXY)$ [60, 67]. The percolation properties of defects in the XY model are also fully analogous to the properties of monopoles: if $\beta < \beta_c$, there is a finite probability that two points are connected by a vortex line if $D = 3$ or by a world surface of a string if $D = 4$, provided that the distance between the investigated points tends to infinity. If $\beta > \beta_c$, this probability is zero. Graphs of the dependences of the fractal dimension of defects on β and on the magnitude of the condensate C on β are given in Refs [60, 67] and they are fully analogous to those shown in Figs 7 and 8. In the region of a phase transition a complete reconstruction of the geometry of clusters formed by defects takes place. We shall describe the properties of clusters which are formed by closed surfaces (world surfaces of strings) on a two-dimensional lattice. If β is close to zero, the probability that a given plaquette belongs to the world surface of a string is approximately 1/6. On a lattice there is an even larger cluster with a multitude of arms and there are also tiny clusters (satellites) which have the topology of a sphere (for simplicity, they will be simply called spheres). The surface of the spheres is of the order of 0.1% of the surface of a large cluster. The individual satellites with a nonzero number of arms (for example, tori) are observed with the probability less than 10^{-5}. The surface area of a large cluster and the number of arms both decrease when β is increased. The situation in the vicinity of a phase transition characterised by $\beta \neq \beta_c$ is as follows. A large percolation cluster is still the only one and its surface area is approximately half that for $\beta = 0$. The satellites have a surface area equal to about 3% of the area of the large cluster. The probability† that among the satellites there is an object with the topology of a torus is approximately 0.1. The situation changes considerably for $\beta > \beta_c$. There is no separate large cluster with the linear dimensions of the order of the lattice size. There are many objects with the topology of a torus and the total area of all the clusters falls rapidly with increase in β.

The numerical characteristics of the cluster geometry can be determined by using the data for the average number of arms. The number of arms g is related to the Euler number

$$N_E = 2 - 2g , \tag{14}$$

† All the probabilities are given for a lattice of size 10^4.

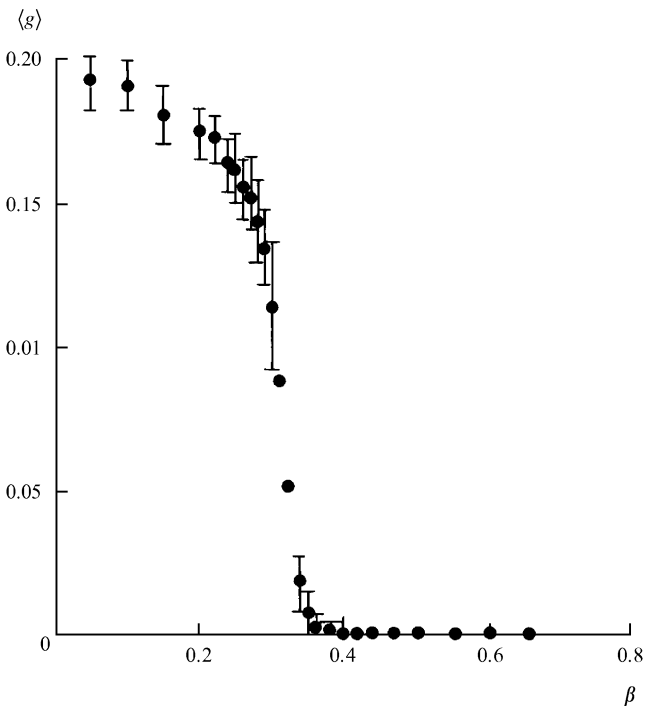

Figure 16. Average number of arms on world surfaces of global strings, weighted in proportion to the areas of these surfaces.

which is easily calculated in our case:

$$N_{\mathrm{E}} = n_{\mathrm{p}} - n_{\mathrm{e}} + n_{\mathrm{s}}\,; \tag{15}$$

here n_{p} is the number of plaquettes, n_{e} is the number of links, and n_{s} is the number of sites forming the investigated surface. Fig. 16, taken from Ref. [60], gives the dependence of the number of arms on the 'reciprocal temperature' β. The number of arms is taken with a weight proportional to the area of a given surface:

$$\langle g\rangle = \frac{\sum_i g_i S_i}{V \sum_i S_i}\,, \tag{16}$$

where the sums in the numerator and denominator are calculated over all the clusters that belong to different configurations of the fields φ, found by the Monte Carlo method for each value of β; g_i is the number of arms in a given cluster; S_i is the surface area of this cluster. A factor inversely proportional to the lattice volume ($V = L^4$) is included to make the results obtained for lattices of different sizes directly comparable. Fig. 16 gives the results of calculations for a lattice of 8^4 size; for each value of β an investigation has been made of 20 statistically independent field configurations. It is evident from this figure that in the 'high-temperature phase' ($\beta < \beta_{\mathrm{c}}$) the surfaces have a nontrivial topology, with a large number of arms, and the quantity $\langle g\rangle$ differs considerably from zero. This behaviour of the surfaces corresponds to zero string tension, leading to the formation of a string condensate when $\beta < \beta_{\mathrm{c}}$.

It therefore follows that an investigation of defects in three-dimensional and four-dimensional XY models shows that below a phase transition ($\beta < \beta_{\mathrm{c}}$) the defects condense, as indicated by their percolation properties, fractal dimension, and geometric structure.

7. Conclusions

This review concentrates on the properties of topological defects, with the exception of Section 2, where a more standard problem of the fractal dimension of domains near a phase transition is considered. In addition to the fractal properties mentioned in the title, the review deals also with the percolation of clusters and their geometric characteristics (the Euler number for the world surfaces of strings). The main conclusion which can be drawn from the reported results is that all these characteristics are highly sensitive to a phase transition and that their behaviour is different in different phases. It can be shown that the main contribution to the condensate C described by the function (7) comes from terms proportional to $1/\beta$ below the phase transition and terms proportional to $\exp(-c\beta)$ above the transition. This behaviour is typical also of the fractal dimensions of defect clusters and of the number of arms on the world surfaces of strings.

There is a well-developed analytic theory of Abelian topological defects (monopoles, vortices, and strings) [20, 59, 60, 68, 69, 70, 71]. In particular, it is possible to write down explicitly the operators representing creation of a topological defect, in spite of the fact that the construction of such nonlocal operators is far from trivial. A brief description of such construction will now be given. It is useful to recall the operator of creation of a charged particle proposed by Dirac [72]. The gauge transformation of the operator of the charged field of matter is $\phi'(x) = \phi(x)\exp[\mathrm{i}\alpha(x)]$. It is possible to propose the following gauge-invariant operator:

$$\phi_{\mathrm{c}}(x) = \phi(x)\exp\left\{\mathrm{i}\int B_k(x-y)A_k(y)\,\mathrm{d}y\right\}. \tag{17}$$

Here, B_k is a Green function such that $\partial_k B_k = \delta(x)$; A_μ is a gauge field which changes as a result of gauge transformations as follows: $A'_\mu(x) = A_\mu(x) + \partial_\mu\alpha(x)$. It is obvious that $\phi_{\mathrm{c}}(x)$ is a *gauge-invariant* operator describing a charge surrounded by a Coulomb cloud of photons. The monopole creation operator can be derived [68, 69] by crossover from compact electrodynamics to a dual theory which represents some limiting case of the Abelian Higgs model. The matter fields now carry a magnetic charge and application of the Dirac formula (17) to these fields, followed by return from the dual to the initial theory, gives the monopole creation operator.

Another example is the creation operator of an Abrikosov–Nielsen–Olesen string in the Abelian Higgs model. A string carries a closed magnetic flux and initially we need to cross over again to the dual theory, which includes gauge and hypergauge fields†. Formation of a Wilson loop $\tilde{W}_C$ from a dual-theory gauge field creates a magnetic flux along a contour C. The operator $\tilde{W}_C$ is gauge-invariant, but not hypergauge-invariant. A derivation similar to that described by the Dirac formula (17) yields a hypergauge-invariant operator in the dual theory. It is shown in Ref. [71] that this operator is the creation operator of an Abrikosov–Nielsen–Olesen string on a contour C. If in this derivation the electric charge is assumed to be zero, the result is the creation operator

† A hypergauge field $h_{\mu\nu} = -h_{\nu\mu}$ is a field whose Lagrangian is invariant under hypergauge transformations $h_{\mu\nu} \to h_{\mu\nu} + \partial_\mu\chi_\nu - \partial_\nu\chi_\mu$, where χ_μ is the hypergauge transformation parameter.

of a global string [70] discussed in Section 6. A more detailed description of analytic approaches to topological defects is outside the scope of this review.

Probably the most useful application of the theory of fractals has been in the study of the mechanism of confinement in SU(2) gluodynamics. The similarity of the properties of monopole currents in SU(2) gluodynamics and in compact electrodynamics shows that in the maximum Abelian projection of the SU(2) theory the confinement is due to a condensate of monopoles and the vacuum has a property similar to a dual superconductor. As pointed out at the end of Section 4, in spite of the fact that the overall confinement scenario is now understood, there are many specific unsolved problems. For example, there is an infinite number of SU(2)→U(1) projections and in the case of some projections the confinement is not due to monopoles, but due to other topological defects (minopoles) [48]. One can consider monopoles of finite size (extended monopoles) and the size of monopoles responsible for the confinement is not yet clear.

Acknowledgements. I am very grateful to A Di Giacomo, T L Ivanenko, J-P Paffuti, A V Pochinskii, Yu A Simonov, J Smit, A I Veselov, and U-J Wiese for valuable discussions. I am also indebted to C Guaraldo, A Selivanov, V G Shevchenko, and Yu A Korzhavin for help with computing technology. I am very greatly indebted to Yi-Cheng Zhang, who was the first to acquaint me with the theory of fractals.

This work was partly financed by the International Science Foundation, Physical Society of Japan (Grant MJM000) and the Russian Fund for Fundamental Research (Grant JSPS). I am grateful to these organisations for their help.

Appendix. Brief introduction to lattice theories

This Appendix gives the main definitions from the theory of a field on a lattice. I am aware that a reader completely unacquainted with lattice theories can find this introduction insufficient and that understanding of the details of this review will require recourse to the book by Creutz [73] or to the review by Makeenko [74]. A reader fully conversant with lattice theories can ignore this Appendix.

The main idea behind the lattice theory is the crossover from an infinite-dimensional functional integral in imaginary time to a finite-dimensional integral. This is done by splitting the four-dimensional (or, in general, D-dimensional) spacetime into a lattice. A lattice in a D-dimensional Euclidean space consists of sites (points), links, plaquettes (unit squares), unit cubes, ..., and D-dimensional unit hypercubes. It is easy to see that on a lattice with periodic boundary conditions the total number of sites is L^D if on each of the coordinate axes there are L sites. Such a lattice has DL^D links (from each site one can see D links in the positive directions), $[D(D-1)/2]L^D$ plaquettes, and $[D(D-1)\ldots(D-d+1)/d!]L^D$ unit objects of the dimension d. Dynamic variables (analogues of continuous fields), which can be numbers or group elements, may be attached to sites, links, plaquettes, etc. The classical (and most elementary) example is the Ising model in which the dynamic variables σ, assuming the values ± 1, are attached to the lattice sites. In general, scalars φ_x are attached to the lattice sites (x is the coordinate of a site). Vectors $U_{x,\mu}$ are attached to links, where x is the coordinate of the beginning of a link and μ is its direction. Antisymmetric tensors, such as the field strength tensor, correspond to plaquettes and have two directions and a coordinate: $\theta_{x,\mu\nu}$.

The action in the theory of a field on a lattice can be described by an expression which, in the limit when the lattice link a tends to zero,† tends to the classical expression for the action. The simplest variant involves replacement of the derivatives with finite differences on a lattice and substitution of the summation over the whole lattice in place of the integration over the whole space. Care is needed in formulation of a gauge theory on a lattice. The problem is this: if a discrete analogue of the continuous action is simply written down, the gauge invariance is lost and this may have serious consequences. For example, gluodynamics then loses the colour confinement property [75, 76].

The initial variant of the lattice action for gauge fields [19, 77] can be written in a gauge-invariant manner:

$$S = \beta\left(1 - \sum_{x,\mu>\nu} \frac{1}{N}\,\mathrm{Re}\,\mathrm{Tr}\,U_{x,\mu\nu}\right). \tag{A.1}$$

Here, the summation is carried out over all the plaquettes, $U_{x,\mu\nu}$ is the plaquette variable,

$$U_{x,\mu\nu} = U_{x,\mu}U_{x+\hat{\mu},\nu}U^{+}_{x+\hat{\nu},\mu}U^{+}_{x,\nu}\,, \tag{A.2}$$

$\hat{\mu}$ is a unit vector directed along the μ axis, and the dynamic variable $U_{x,\mu}$ attached to a lattice link is an $N\times N$ matrix and belongs to the gauge group representation G. The relationship with the gauge field $\hat{A}_\mu$, which corresponds to the algebra of G, is

$$U_{x,\mu} = \exp\left[\mathrm{i}ag\hat{A}_\mu(x)\right]\,, \tag{A.3}$$

where g is the unrenormalised charge in this theory.

If the above expression is substituted in formula (A.1), if the term leading in a is retained, and if summation is replaced with integration, then for $\beta = 2N/g^2$ the action is

$$\begin{aligned} S &= \frac{1}{2}\int \mathrm{Tr}\,\hat{F}^2_{\mu\nu}\,\mathrm{d}^4x + O(a^6)\,,\\ \hat{F}_{\mu\nu} &= \partial_\mu\hat{A}_\nu - \partial_\nu\hat{A}_\mu - \mathrm{i}g[\hat{A}_\mu,\hat{A}_\nu]\,, \end{aligned} \tag{A.4}$$

i.e. the lattice action of formula (A.1) reduces in the continuous limit to the standard action of gauge fields.

The generating functional in quantum gluodynamics is

$$\mathcal{Z} = \int \mathrm{D}U\exp(-S)\,, \tag{A.5}$$

where $\mathrm{D}U = \prod_{x,\mu}\mathrm{d}U_{x,\mu}$ is the integral over all the dynamic variables. The action S described by formula (A.1) is invariant under the gauge transformations

$$U'_{x,\mu} = \Omega_x U_{x,\mu}\Omega^{+}_{x+\mu}\,, \tag{A.6}$$

where Ω_x is a matrix of gauge transformations attached to a site x. Formula (A.5) is gauge invariant if the integration measure has the following properties: $\mathrm{d}U_{x,\mu} = \mathrm{d}U_{x,\mu}V_1 = \mathrm{d}V_2U_{x,\mu}$, for arbitrary values of V_1 and V_2, i.e. $\mathrm{d}U_{x,\mu}$ is

† In this review the system of units is that generally employed and characterised by $a = 1$, if it does not hinder understanding of the subject in hand. Sometimes, for the sake of clarity, a is left in the formulas.

the Haar measure for the group G. In the continuum limit ($a \to 0$), application of formula (A.3) readily demonstrates that formula (A.6) describes an ordinary gauge transformation:

$$A_\mu \to \Omega^+ A_\mu \Omega + \frac{\mathrm{i}}{g}\,\Omega^+ \partial_\mu \Omega\,.$$

The action described by formula (A.1) is not unique: there is an infinite number of gauge-invariant actions on a lattice which in the continuum limit reduce to the Yang–Mills action. It is not a trivial result that in the quantum continuum limit all the numerically investigated actions have the same (within the limits of statistical errors) effect in quantum gluodynamics. This property of 'universality' can be demonstrated theoretically for gluodynamics with a large number of colours [78].

One of the main motives for the formulation of lattice gauge series has been the hope of obtaining physical results in the form of a series in terms of the reciprocal charge $(1/g)$ and not as a standard perturbation-theory series in terms of g. The existence of the confinement of colour charges has been demonstrated [19] in the leading order of the strong-coupling expansion in terms of $1/g$. Subsequent theoretical and numerical investigations have led to the conclusion that this result probably does not apply in the continuum limit. Nevertheless, it has proved that the lattice formulation makes it possible to obtain physical results (at least when supercomputers are used). In reality, up to the early eighties it has been difficult to see how the Feynman path integral in field theory can be investigated numerically. The unexpected success achieved by Creutz (as described in his book [73] and in the literature there) in the generation of lattice gauge theories by the Monte Carlo method has created a new trend in the physics of strong interactions, which is numerical simulation of quantum chromodynamics. The decisive technical aspect has been the use of the Monte Carlo method, which involves the following operations.†

Let us assume that we need to calculate a quantity (which is an analogue of a quantum average)

$$\langle F(U)\rangle = \frac{\int F(U)\exp[-S(U)]\,\mathrm{d}u}{\int \exp[-S(U)]\,\mathrm{d}u}\,, \tag{A.7}$$

where $\int \mathrm{d}u$ is a finite-dimensional integral. If points are scattered at random over the integration domain (one set of points U_i is called a configuration), then

$$\langle F(U)\rangle \approx \frac{\sum_{i=1}^{N} F(U_i)\exp\left[-S(U_i)\right]}{\sum_{i=1}^{N} \exp\left[-S(U_i)\right]}\,, \tag{A.8}$$

where the equality corresponds to the limit in which the number of configurations N tends to infinity. The proposed procedure may prove extremely slowly converging in numerical calculations. The reason for this is the presence of an exponential function in the sums in formula (A.8), but for random U_i the majority of configurations will be exponentially suppressed. The convergence can be improved by scattering the configurations so that their distribution is characterised by the following probability density:

$$\rho(U) = \frac{\exp\left[-S(U)\right]}{\int \exp\left[-S(U)\right]\,\mathrm{d}u}\,, \tag{A.9}$$

where we now have

$$\langle F(U)\rangle \approx \frac{1}{N}\sum_{i=1}^{N} F(U_i)\,, \tag{A.10}$$

and there are no exponentially small factors. This method can be used to carry out calculations on sufficiently large lattices: for example, Fig. 14 in Section 5 is derived for the SU(2) gluodynamics on a lattice of $24^3 \times 40$ size; the number of links on this lattice is $N_1 = 4 \times 24^3 \times 40$ and a triple integral is calculated for each link [because there are three group SU(2) generators]. This gives an integral of multiplicity $3N_1 = 6\,635\,520$. Integrals of this multiplicity have been calculated successfully not only because of application of the thoroughly tested Monte Carlo methods, but also because the physically interesting quantities are not strongly nonlocal and are averaged over the whole volume of the lattice.

The first question which arises in an analysis of the numerical data is: how are the results obtained related to the continuum limit? The continuum limit is that at which the discrete structure of a lattice is no longer felt and the finite volume of the lattice has no influence. From the point of view of lattice theory such a limit should correspond to the points at which second-order phase transitions occur. On approach to these points the correlation length ξ tends to infinity when expressed in lattice units: $\xi/a \to \infty$ (a is the length of a lattice link), so that the physical quantities expressed in terms of ξ are insensitive to the lattice step a; in other words, we have effectively the situation in which $a \to 0$. The length of a lattice link in the SU(N) lattice gauge theory when the unrenormalised charge g is sufficiently small can be described as follows in terms of the lattice truncation parameter Λ_L:

$$a = \frac{1}{\Lambda_L}\left[\frac{24\pi^2}{11}\,\frac{\beta}{N^2}\right]^{51/121} \exp\left\{-\frac{12\pi^2}{11}\,\frac{\beta}{N^2}\right\}, \qquad \beta = \frac{2N}{g^2}\,. \tag{A.11}$$

This expression is simply a two-loop variant of the expression for asymptotic freedom:

$$g^2 = \frac{1}{c\ln(p/\Lambda)}\,,$$

where instead of the external momentum p we have the reciprocal of the length of a lattice link $1/a$. It is evident from formula (A.11) that $a \to 0$ when $g \to 0$, i.e. the continuum limit of the theory is reached. However, numerical calculations cannot be carried out for a value of g which is too small since, in order to have a finite physical volume of the lattice ($V = L^4 a^4$), we need to consider lattices with increasing numbers of sites ($L \propto 1/a$) on approach to the limit $a \to 0$. However, the number of the dynamic variables (proportional to L^4) is limited by the computer power. This leads to the problem of determina-

† The idea of applying stochastic methods to solve the Schrödinger equation was evidently first put forward by Fermi, who pointed out that the equation for diffusion with absorption is equivalent to the Schrödinger equation in imaginary time. Fermi was then engaged on the Los Alamos Project, where von Neumann was also working, and the latter proposed the excellent Monte Carlo method for the calculation of neutron scattering. Fermi's comment had not been published but it is mentioned in Ref. [79].

tion of whether the continuum limit has been reached in a specific calculation. Since the only dimensional parameter in this theory is the length of a lattice link, the dimensional quantities are expressed only in terms of this length.

The simplest and the most thoroughly investigated physical quantity found by numerical simulation of lattice gauge theories is what is known as the string tension σ. This quantity determines the force of interaction between a quark and an antiquark, both of which are infinitely heavy and are separated by an infinite distance. Since the action defined by formula (A.1) and the generating functional of formula (A.5) do not contain dimensional quantities in gluodynamics, numerical calculations are used to find not the string tension σ but the dimensionless quantity $\chi = \sigma a^2$. Thanks to formula (A.11), the dependence of χ on the unrenormalised charge g is known in the continuum limit and such a dependence has indeed been observed in numerical experiments. The procedure described above represents a standard check for the existence of the continuum limit in lattice theories [73].

Topological defects, which are monopoles, vortices, and strings, are discussed in Sections 3–6 above. We shall now consider the simplest topological defect which appears in the XY model. In this model the action is.

$$S = \beta \sum_{x,\mu} \cos(\varphi_x - \varphi_{x+\hat{\mu}}) \,, \tag{A.12}$$

where the constant β represents the reciprocal of temperature; the summation is carried out over all the lattice links, which are defined by a site x and a direction μ; the dynamic variables φ_x, defined at the lattice sites, are compact: $-\pi < \varphi_x \leqslant \pi$. The cosine in formula (A.12) can be replaced by any 2π-periodic function because this does not affect in any qualitative way the dynamic properties of the model. There are topological excitations in this model and they are defined as follows. Let us consider an elementary plaquette (Fig. 15) and let us assume that compact dynamic variables φ_i $(i = 1, \ldots, 4)$ are attached to the sites of this plaquette. Let us calculate the quantity

$$\begin{aligned} {}^*j = \frac{1}{2\pi} \big(& [\varphi_1 - \varphi_2]_{2\pi} + [\varphi_2 - \varphi_3]_{2\pi} \\ & + [\varphi_3 - \varphi_4]_{2\pi} + [\varphi_4 - \varphi_1]_{2\pi} \big) \,, \end{aligned} \tag{A.13}$$

where $[\alpha]_{2\pi}$ denotes calculation of the quantity α modulo 2π:

$$[\alpha]_{2\pi} = \alpha + 2\pi p \,, \qquad -\pi < (\alpha + 2\pi p) \leqslant \pi \,.$$

It therefore follows that links 12, 23, 34, and 41 correspond to integral variables $p_1, \ldots, p_4$, in terms of which ${}^*j$ can be expressed as follows:

$${}^*j = p_1 + p_2 + p_3 + p_4 \tag{A.14}$$

If ${}^*j \neq 0$, we can say that there is a dislocation which in the two-dimensional model should be attributed to the centre of the investigated plaquette. In the three-dimensional model a dislocation should be attributed to a link in a dual lattice† and this link is perpendicular to the plaquette and passes through its centre. In the four-dimensional space a dislocation is attributed to a plaquette in a dual lattice which is perpendicular to the initial plaquette and passes through its centre. Therefore, a dislocation is on a dual lattice and we shall use the notation ${}^*j$ and not simply j.

Therefore, from a given configuration of fields φ we can select dislocations of ${}^*j$. The currents ${}^*j$ have two remarkable properties. First, there is a law of conservation as a result of which the lines formed on a dual lattice by the currents ${}^*j$ are closed in the three-dimensional model. In the four-dimensional model the currents ${}^*j$ form closed surfaces. This law of conservation is the lattice analogue [60, 70] of the law of conservation of the current corresponding to a topological defect.

For $D = 3$, the dislocations of ${}^*j$ are vortices similar to the vortices in superfluid helium and for $D = 4$ the plaquettes on a dual lattice with ${}^*j \neq 0$ are the world surfaces of closed 'global strings' [58]. The physical meaning of ${}^*j$ is discussed in greater detail in Section 6.

A second important property of ${}^*j$ is the topological nature of the excitations which lead to ${}^*j \neq 0$. This is obvious if only because the integral number of ${}^*j$ can be derived from continuous variables φ_i. This means that a sufficiently small but finite variation of φ_i does not alter ${}^*j$, i.e. ${}^*j$ is a topological charge. The explicit example in Fig. 15 is as follows: $\varphi_1 = \varphi_2 = 0$, $\varphi_2 = -\varphi_3 = -\pi + \delta$, then ${}^*j = 1$, if $0 < \delta < \pi/2$.

A striking illustration of the connection between a topological defect and a physical effect is the role of vortices in the dynamics of a phase transition in the two-dimensional XY model [20, 61, 62]. In Section 6 we discussed the properties of vortices in the three-dimensional and four-dimensional XY models. The monopoles discussed in Sections 3–5, like the vortices, are topological defects in Abelian theories. The only difference is that the vortices are formed from variables ϕ attached to the lattice sites and monopoles are formed from vector fields attached to the lattice links. There is a formalism of differential forms on a lattice [59, 60, 70] which can be used to describe topological defects in a universal manner.

† A dual lattice is defined as follows. The initial lattice is displaced by half a step $(a/2)$ along the positive direction of axis 1, axis 2, ..., axis D. In this way the sites in the dual lattice are at the centres of elementary D-dimensional hypercubes of the original lattice.

References

1. Mandelbrot B B *The Fractal Geometry of Nature* (San Francisco: W H Freeman, 1982)
2. Paladin G, Vulpiani A *Phys. Rep.* **156** 147 (1987)
3. Yi-Cheng Zhang, Serva M, Polikarpov M *J. Stat. Phys.* **58** 849 (1990)
4. Gross D J, Wilczek F *Phys. Rev. Lett.* **30** 1343 (1973)
5. Politzer H D *Phys. Rev. Lett.* **30** 1346 (1973)
6. Weinberg S *Phys. Rev. Lett.* **31** 494 (1973)
7. Bali G S, Schilling K, Schlichter C, Preprint CERN-TH.7413/94 (Geneva: Cern, 1994)
8. 't Hooft G, in *High Energy Physics* (Ed. M Zichichi) (Bologna: Editrice Compositori, 1976)
9. Mandelstam S *Phys. Rev. C* **23** 245 (1976)
10. Abrikosov A A *Zh. Eksp. Teor. Fiz.* **32** 1442 (1957) [*Sov. Phys. JETP* **5** 1174 (1957)]
11. Wiese U-J, Polikarpov M I *Pis'ma Zh. Eksp. Teor. Fiz.* **51** 296 (1990) [*JETP Lett.* **51** 336 (1990)]
12. Polikarpov M I *Phys. Lett. B* **236** 61 (1990)
13. Engels J, Karsch F, Satz H, Montvay I *Nucl. Phys. B* **205** [FS5] 545 (1982)
14. Kuti J, Polonyi J, Szlachanyi K *Phys. Lett. B* **98** 199 (1981)
15. Polyakov A M *Phys. Lett. B* **72** 477 (1978)
16. Domb C *J. Phys. A* **9** L17 (1976)
17. Binder K *Ann. Phys.* **98** 390 (1976)

18. Cambier J L, Nauenberg M *Proceedings of Sixth Trieste International Symposium on Fractals in Physics (ICTP '85), Trieste, 1985* (Eds L Pietronero, E Tosatti) (Amsterdam: North-Holland, 1986)
19. Wilson K G *Phys. Rev. D* **10** 2445 (1974)
20. Polyakov A M *Gauge Fields and Strings* (New York: Harwood, 1987)
21. Banks T, Myerson R, Kogut J *Nucl. Phys. B* **129** 493 (1977)
22. Cardy J L *Nucl. Phys. B* **170** [FS1] 369 (1980)
23. DeGrand T A, Toussaint D *Phys. Rev. D* **22** 2478 (1980)
24. Kronfeld A S, Schierholz G, Wiese U-J *Nucl. Phys. B* **293** 461 (1987)
25. Kronfeld A S, Laursen M L, Schierholz G, Wiese U-J *Phys. Lett. B* **198** 516 (1987)
26. Polley L, Polikarpov M I, Wiese U-J *Phys. Lett. B* **253** 212 (1991)
27. Ivanenko T L, Polikarpov M I, Pochinskii A V *Pis'ma Zh. Eksp. Teor. Fiz.* **53** 517 (1991) [*JETP Lett.* **53** 543 (1991)]
28. Ivanenko T L, Pochinsky A V, Polikarpov M I *Phys. Lett. B* **302** 458 (1993)
29. Essam J W, in *Phase Transitions and Critical Phenomena* (Eds C Domb, M S Green) (New York: Academic Press, 1972) Vol. 2
30. Grimmett G *Percolation* (Berlin: Springer, 1989)
31. 't Hooft G *Nucl. Phys. B* **190** [FS3] 455 (1981)
32. Suzuki T *Proceedings of the International Symposium on Lattice Field Theory (Lattice '92), Amsterdam, 1992*, in *Nucl. Phys. B (Proc. Suppl.)* **30** 176 (1993)
33. Suzuki T, Yotsuyanagi I *Phys. Rev. D* **42** 4257 (1990)
34. Bornyakov V G, Ilgenfritz E-M, Laursen M L, et al. *Phys. Lett. B* **261** 116 (1991)
35. Singh V, Browne D, Haymaker R *Phys. Lett. B* **306** 115 (1993)
36. Shiba H, Suzuki T, Preprint 94-07 (Kanazawa, Japan: Kanazawa University, 1994)
37. Stack J D, Neiman S D, Wensley R J, Preprint ILL-(TH)-94-14 (Urbana-Champaign, IL: Dept. of Physics, Illinois University, 1994)
38. Shiba H, Suzuki T, Preprint 94-12 (Kanazawa, Japan: Kanazawa University, 1994)
39. Ivanenko T L, Polikarpov M I, Pochinsky A V *Phys. Lett. B* **252** 631 (1990)
40. Kitahara S, Matsubara Y, Suzuki T, Preprint 94-24 (Kanazawa, Japan: Kanazawa University, 1994)
41. Kanaya K, Satz H *Phys. Rev. D* **34** 3193 (1986)
42. Berg B *Phys. Lett. B* **104** 475 (1981)
43. Iwasaki Y, Yoshie T *Phys. Lett. B* **127** 197 (1983)
44. Teper M *Phys. Lett. B* **162** 357 (1985)
45. Ilgenfritz E M, Laursen M L, Muller-Preussker M, et al. *Nucl. Phys. B* **268** 693 (1986)
46. Campostrini M, Di Giacomo A, Maggiore M, et al. *Phys. Lett. B* **225** 403 (1989)
47. Polikarpov M I, Veselov A I *Nucl. Phys. B* **297** 34 (1988)
48. Chernodub M N, Polikarpov M I, Veselov A I *Phys. Lett. B* **342** 303 (1995)
49. Chernodub M N, Polikarpov M I, Zubkov M A *Proceedings of International Symposium on Lattice Field Theory (Lattice '93), Dallas, TX, 1993*, in *Nucl. Phys. B (Proc. Suppl.)* **34** 256 (1994)
50. Polikarpov M I, Chernodub M N *Pis'ma Zh. Eksp. Teor. Fiz.* **59** 439 (1994) [*JETP Lett.* **59** 459 (1994)]
51. Smit J, van der Sijs A *Nucl. Phys. B* **355** 603 (1991)
52. 't Hooft G *Nucl. Phys. B* **79** 276 (1974)
53. Polyakov A M *Pis'ma Zh. Eksp. Teor. Fiz.* **20** 430 (1974) [*JETP Lett.* **20** 194 (1974)]
54. Bogomol'nyi E B *Yad. Fiz.* **24** 861 (1976) [*Sov. J. Nucl. Phys.* **24** 449 (1976)]
55. Prasad M K, Sommerfield C M *Phys. Rev. Lett.* **35** 760 (1975)
56. Polikarpov M I, Yee K *Phys. Lett. B* **333** 452 (1994)
57. Polikarpov M I, Yee K, Zubkov M A *Phys. Rev. D* **48** 3377 (1993)
58. Vilenkin A *Phys. Rep.* **121** 263 (1985)
59. Ivanenko T L, Polikarpov M I, Preprint ITEP-49 (Moscow: Institute of Theoretical and Experimental Physics, 1991)
60. Bukenov A K, Wiese U-J, Polikarpov M I, Pochinskii A V *Yad. Fiz.* **56** 214 (1993) [*Phys. At. Nucl.* **56** 122 (1993)]
61. Berezinskii V L *Zh. Eksp. Teor. Fiz.* **59** 907 (1970) [*Sov. Phys. JETP* **32** 493 (1971)]
62. Kosterlitz J M, Thouless D J *J. Phys. C* **6** 1181 (1973)
63. Onsager L *Nuovo Cimento* **6** 279 (1949)
64. Feynman R P *Prog. Low Temp. Phys.* **1** 17 (1955)
65. Williams G A *Phys. Rev. Lett.* **59** 1926 (1987); Erratum **61** 1142 (1988)
66. Shenoy S R, Preprint (Karlsruhe, Germany: Universitat Karlsruhe, 1989)
67. Pochinsky A V, Polikarpov M I, Yurchenko B N *Phys. Lett. A* **154** 194 (1991)
68. Frohlich J, Marchetti P A *Europhys. Lett.* **2** 933 (1986)
69. Frohlich J, Marchetti P A *Commun. Math. Phys.* **112** 343 (1987)
70. Polikarpov M I, Wiese U-J, Preprint HLRZ 90-78 (Julich, Germany: Hochstleistungsrechenzentrum, KFA, 1990)
71. Polikarpov M I, Wiese U-J, Zubkov M A *Phys. Lett. B* **309** 133 (1993)
72. Dirac P A M *Can. J. Phys.* **33** 650 (1955)
73. Creutz M *Quarks, Gluons and Lattices* (Cambridge: Cambridge University Press, 1985)
74. Makeenko Yu M *Usp. Fiz. Nauk* **143** 161 (1984) [*Sov. Phys. Usp.* **27** 401 (1984)]
75. Patrascioiu A, Seiler E, Stamatescu I O *Phys. Lett. B* **107** 364 (1984)
76. Seiler E, Stamatescu I O, Zwanziger D *Nucl. Phys. B* **239** 177 (1984)
77. Polyakov A M *Phys. Lett. B* **59** 79 (1975)
78. Makeenko Yu M, Polikarpov M I *Nucl. Phys. B* **205** [FS5] 386 (1982)
79. Metropolis N, Ulam S *J. Am. Stat. Assoc.* **247** 335 (1949)